

Doppler SD-OCT
blood flow analysis and extraneous
operator influences

by

Chitman Uppal

A thesis
presented to the University of Waterloo
in fulfillment of the
thesis requirement for the degree of
Master of Science
in
Vision Science

Waterloo, Ontario, Canada, 2014

© Chitman Uppal 2014

AUTHOR'S DECLARATION

I hereby declare that I am the sole author of this thesis. This is a true copy of the thesis, including any required final revisions, as accepted by my examiners.

I understand that my thesis may be made electronically available to the public.

Abstract

Purpose: The RTVue-100 is a new instrument for measuring retinal blood flow (RBF), but image quality needs to be optimized in order for valid blood flow results. The primary aim of this thesis was to assess the presence of learning effects with novice and experienced operators. **Methods:** Twelve upper-year optometric students from the University of Waterloo, School of Optometry and Vision Science, were trained in operating RTVue-100. Nine healthy participants, with a mean age (\pm SD) of 25.7 ± 3.8 years, underwent OCT imaging. Using the Doppler OCT of Retinal Circulation (DOCTORC) software, images were assessed by computer for various image quality parameters. **Results:** Paired samples t-tests showed significant statistical differences between the novice and experienced operators for the following image acquisition parameters: total acquisition time (TAT), number of attempts to complete total scan protocol, and number of valid images. Mean values for TAT and the number of attempts decreased, whereas the mean number of valid images increased from novice to experienced level. **Conclusions:** The results confirm that there are learning effects observed within the image acquisition process using the RTVue-100 SD-OCT.

Acknowledgements

I would like to express my sincere appreciation for my supervisor, Dr. Trefford Simpson, whose guidance and mentoring enhanced my experience in graduate school.

I would like to thank my committee members, Dr. Vivian Choh and Dr. Kostadinka Bizheva, for their extensive care and support throughout all aspects of the thesis. I would like to also thank my professors, Dr. Christopher Hudson and Dr. John Flanagan, for their teachings.

I am very grateful for my close friends of the Graduates in Vision Science (GIVS) for being resourceful and encouraging during my studies.

Indeed, this accomplishment would not be possible without the participation of volunteers in the study. Thank you to all the study volunteers for their assistance and contribution of time towards furthering our knowledge of vision science.

My sources of funding have been granted by the Ontario Research Fund (ORF) and the Canadian Optometric Education Trust Fund (COETF).

Dedication

I dedicate my thesis to my parents Balbir and Manjit Singh. Thank you for being proud of me and giving me the opportunity to pursue my dreams.

Thank you to my brilliant brother Gurman Singh for his motivation.

Table of Contents

AUTHOR’S DECLARATION	ii
ABSTRACT.....	iii
ACKNOWLEDGEMENTS	iv
DEDICATION.....	v
TABLE OF CONTENTS	vi
LIST OF FIGURES	ix
LIST OF TABLES	xi
LIST OF ABBREVIATIONS	xii
Chapter 1 Literature Review: Learning Effect, OCT, and Retinal Blood Flow.....	1
1.1 Introduction	1
1.1.1 Assessment of Learning Effects in Imaging Techniques.....	2
1.1.2 Assessment of Learning Effects in Clinical Studies	3
1.2 Assessment of Learning Effects in Psychophysical Studies	3
1.3 Optical Coherence Tomography	5
1.3.1 Principle of OCT.....	5
1.3.2 Comparison of Commercial OCT Devices	6
1.3.3 RTVue-100 Spectral Domain Optical Coherence Tomography.....	7
1.4 Anatomy of Retinal Blood Circulation	8
1.4.1 The Retinal Microvasculature.....	9
1.4.2 Blood-Retinal Barrier.....	10
1.5 Retinal Blood Flow Regulation.....	10
1.5.1 Mechanisms of Autoregulation.....	11
1.6 Blood Flow Dynamics.....	12
1.6.1 Ohm’s Law.....	12
1.6.2 Poiseuille’s Law	13
1.6.3 Arterial Blood pressure	13
1.6.4 Inner and Outer Pressures of the eye	13
1.7 Conclusion.....	14
Chapter 2 Rationale.....	15

2.1	Introduction	15
2.2	Aims	15
2.3	Hypotheses	16
2.4	Conclusion.....	16
Chapter 3 Materials and Methods.....		17
3.1	Introduction	17
3.2	Sample Size determination.....	17
3.3	Number of Participants estimation.....	17
3.4	Justification for the recruitment of Doctor of Optometry (OD) students.....	18
3.5	Definition of a novice and experienced operator	18
3.6	Inclusion criteria for novice and experienced operator	18
3.7	Imaged participants	19
3.8	Procedures	19
3.8.1	Visits	19
3.8.2	Image Acquisition Protocol	20
3.8.3	Training Protocol	23
3.8.4	Quantitative Assessment of Image Acquisition Parameters	25
3.8.5	Statistical Analysis.....	26
3.9	Conclusion.....	27
Chapter 4 Results.....		28
4.1	Introduction	28
4.2	Imaged participant characteristics	28
4.3	Tests for Normality of Data	29
4.4	Image Acquisition Parameters	29
4.4.1	Total Acquisition Time	29
4.4.2	Number of Attempts	33
4.4.3	Number of Valid Images.....	36
4.4.4	Relationship between image acquisition parameters	38
4.5	Conclusion.....	41
Chapter 5 General Discussion.....		42

References	46
Copyright permissions.....	59
Nature Publishing Group	59
Pilot Study	63

List of Figures

Figure 1.1 Diagram of anatomy of the ophthalmic artery	9
Figure 3.1 The detailed procedures for session.....	20
Figure 3.2 RTVue Participant Fixation Chart.....	22
Figure 3.3 Image Quality Check	23
Figure 3.4 Operating controls for the RTVue-100.....	24
Figure 3.5 Supranasal Doppler Scan Position.....	24
Figure 3.6 RTVue Training Checklist.....	25
Figure 3.7 Study Design.....	27
Figure 4.1 Histogram of Difference in TAT with Normal Distribution Curve.....	29
Figure 4.2 Line graph of the average Total Acquisition Time.....	31
Figure 4.3 Box plot of Total Acquisition Time	31
Figure 4.4 Scatter plot of the difference in Total Acquisition Time.....	32
Figure 4.5 Frequency distribution histogram for Total Acquisition Time.....	32
Figure 4.6 Histogram for the difference in Total Acquisition Time	33
Figure 4.7 Line graph of the average number of attempts	34
Figure 4.8 Scatter plot of the difference in Number of Attempts	35
Figure 4.9 Frequency distribution histogram for Number of Attempts.	35
Figure 4.10 Histogram for the difference in Number of Attempts	36

Figure 4.11 Line graph of the average number of valid images 37

Figure 4.12 Frequency distribution histogram for Number of Valid Images. 38

Figure 4.13 Histogram for the difference in Number of Valid Images..... 38

Figure 4.14 Line graph of the ratio of TAT and Number of Attempts. 39

Figure 4.15 Line graph of the average time per image acquisition..... 40

List of Tables

Table 1.1 Comparison of Commercial Optical Coherence Tomography Devices.....	7
Table 4.1 Imaged participant characteristics.....	28
Table 4.2 Differences in Image Acquisition Parameters by Experience Level	41

List of Abbreviations

AMD.....	Age-related macular degeneration
ANSI.....	American National Standards Institute
BM.....	Bruch's membrane
BP.....	Blood pressure
BPOMA.....	Balance performance oriented mobility assessment
CAS.....	Carotid artery stenting
CCT.....	Central corneal thickness
CNS.....	Central nervous system
CO ₂	Carbon dioxide
CRA.....	Central retinal artery
DC.....	Dioptres cylinder
DOCTORC.....	Doppler optical coherence tomography of retinal circulation
DS.....	Dioptres sphere
EDCF.....	Endothelial derived constricting factor
EDRF.....	Endothelial specific derived relaxing factor
ET.....	Endothelin
EVH.....	Endoscopic vein harvesting
FDA.....	Food and drug administration
η.....	Viscosity
HD-OCT.....	High-definition optical coherence tomography
IOP.....	Intra-ocular pressure

IR.....	Infrared
K-S.....	Kolmogorov-Smirnov
L.....	Length
LDF.....	Laser Doppler flowmetry
MBSS.....	Modified barium swallow studies
MPI.....	Myocardial perfusion imaging
NO.....	Nitric oxide
O ₂	Oxygen
oBRB.....	Outer blood retinal barrier
OCT.....	Optical coherence tomography
OD.....	Doctor of optometry
ONH.....	Optic nerve head
OPP.....	Ocular perfusion pressure
ΔP.....	Pressure gradient
pO ₂	Arterial oxygen tension
Q.....	Flow
r.....	Radius
R.....	Resistance
RBF.....	Retinal blood flow
RE.....	Refractive error
RNFL.....	Retinal nerve fiber layer
RPE.....	Retinal pigment epithelium
SD.....	Standard deviation

SD-OCT.....	Spectral-domain optical coherence tomography
SNR.....	Signal-to-noise ratio
SSI.....	Signal strength index
SS-OCT.....	Swept-source optical coherence tomography
TAT.....	Total acquisition time
TD-OCT.....	Time-domain optical coherence tomography
UGRA.....	Ultrasound-guided regional anesthesia
VR.....	Virtual reality

Chapter 1

Literature Review: Learning Effect, OCT, and Retinal Blood Flow

1.1 Introduction

A “Learning Effect” is a quantified unit of performance measured over a given number of repetitions. Learning effect differs from learning in general which is the ability to acquire new, or modify and reinforce, existing knowledge and skills. The theory of a learning effect can be found in various fields of study. Specific areas of interest include surgical training, clinician trials, imaging techniques, and perceptual learning. Investigating the influence of learning effects is important to our understanding of how extraneous factors can affect scientific results. Learning effects could affect results in Optical Coherence Tomography (OCT) imaging and data analysis as previous literature suggests that through training operators are able to produce more accurate blood flow results. In recent years, the RTVue-100, a commercial OCT has been used to image ocular tissue. Although it is often relatively simple to operate a commercial OCT instrument, the operator might need to have some knowledge of the anatomy and physiology of the retina in order to capture accurate images and analyze these images properly.

The theory of a learning effect was first experimentally shown by the nineteenth century German psychologist Hermann Ebbinghaus. The theory of learning effect states that the more times a procedure has been completed, there will be more improvement in performance per subsequent iteration. Ramsay et al⁽⁸¹⁾ suggest that many health technologies exhibit some form of learning effect, and this represents a challenge to rigorous assessment. The functioning of health technologies changes with time, more so earlier⁽⁷⁶⁾ as operators become more experienced and confident.

The assessment of learning curves has been conducted in numerous branches of medicine, including surgery. For example, Kiani et al⁽⁶⁸⁾ stated “endoscopic vein harvesting (EVH) by

novice harvesters resulted in a greater number of discrete graft injuries and greater expression of tissue-injury genes than EVH done by experienced”. The results from another study, conducted by Bali et al⁽⁶⁵⁾, demonstrated that surgeons who had prior experience with the use of femtosecond lasers in refractive surgery initially compared to non-refractive surgeons were more comfortable using this technology. The average number of docking attempts progressively decreased as the surgeons’ experience increased. Carotid artery stenting, a procedure used in vascular surgery, requires vigorous operator training because improved performance is closely tied with a decrease in complication rates⁽⁷⁰⁾. Learning curve assessments via virtual reality (VR) simulation have become an integral part of training for medical residents. Results from VR assessment studies generally indicate a shift of learning from the simulation laboratory to the clinic⁽⁹⁴⁾. This form of training may be a potential means to avoid possible risks of novice laparoscopic surgery⁽⁶⁰⁾. Also, simulation training has been found to improve the accuracy in performing both ultrasound-guided regional anesthesia (UGRA) in novice anesthesia residents⁽⁶⁹⁾ and cataract surgery in surgical residents⁽⁶³⁾. Overall, medical training via simulation has become effective in enhancing the quality of care offered by physicians⁽⁹⁵⁾.

1.1.1 Assessment of Learning Effects in Clinical Studies

There have also been clinical studies observing learning effects within clinician-patient interactions. For instance, with minor training many physical therapists can achieve more accurate results when applying Tinetti’s Balance Performance Oriented Mobility Assessment (BPOMA) in an elderly population⁽⁶⁶⁾. Bonilha et al⁽⁶⁴⁾ found that in modified barium swallow studies (MBSS) by novice clinicians had longer radiation exposure times when compared to those of experienced clinicians. A longitudinal qualitative study, conducted by Frankel et al⁽⁹³⁾, concluded “effective use of computers in the outpatient exam room may be dependent upon

clinicians' baseline skills that are carried forward and are amplified, positively or negatively, in their effects on clinician-patient communication". More studies are needed on the impact of novel technologies on the clinician-patient interaction as studies up until now have utilized older techniques.

1.1.2 Assessment of Learning Effects in Imaging Techniques

The assessment of learning effects has offered an understanding of the training of operators in the use of imaging instruments. A combination of unique scan patterns and exclusive deviation analysis makes the RTVue a powerful early glaucoma detection and management learning tool. Filipucci et al⁽⁶¹⁾ state "a novice operator can obtain acceptable sonographic images in 24 non-consecutive hours of active scanning after an intensive self-teaching programme". Fathi et al⁽⁶⁷⁾ found that the incorporation of myocardial tissue Doppler velocity in the identification of heart disease increased the reliability of inexperienced and experienced echocardiographic imaging, but no improvements were observed in expert echocardiographers. A similar study⁽⁸³⁾, investigating learning in myocardial perfusion imaging (MPI), revealed that novice operators can produce similar results as experts after adequate training and quality assurance was provided. More studies are needed on the impact of training of operators in the use of novel imaging instruments as studies up until now have utilized older techniques.

1.2 Assessment of Learning Effects in Psychophysical Studies

Practice can improve performance on a variety of visual tasks, including perceptual learning in foveal and peripheral vision. A review on psychophysical studies⁽¹¹⁰⁾ comparing learning effects across different tasks indicates that a variety of factors affect learning, including the number of perceptual dimensions relevant to the task, external noise, familiarity, and task complexity. For instance, more complex tasks that required discriminations along more than one perceptual

dimension showed more learning, whereas tasks involving simple stimuli and judgements along a single perceptual dimension tended to show only small amounts of learning. Significant learning can occur for both vernier and resolution acuity in majority of individuals, with significant individual differences in the degree and time-course of learning⁽¹¹¹⁾. McKee and Westheimer⁽¹¹²⁾ showed that in the fovea the ability to judge whether or not two lines are perfectly aligned improves by 40% after 2000-2500 trials of practice. Studying perceptual learning is important to our understanding of the limitations of peripheral vision in relation to reading. In macular diseases where central vision is lost, such as age-related macular degeneration, people must rely on their peripheral vision to read. It has been shown that practice in identifying letters can lead to an improvement in peripheral reading speed⁽¹¹³⁾.

It is important to note that although training can improve performance levels, the process of repetition can also induce learning effects. Chung et al⁽¹¹³⁾ showed that through repetitive testing on observers who did not receive training, this repetition can effectively provide these individuals with sufficient training to approach the improved performance levels of trained observers. This study also indicated that even after the training ceases, observers who received training retain most of their improvements for at least three months. The time course of learning a visual skill has also been investigated. Karni and Sagi⁽¹¹⁴⁾ suggest that observers learning a visual task showed little or no improvement until up to 8 hours after training, but large improvements occurred thereafter. There was almost no forgetting in observers learning this visual task and improvements that were gained were retained for at least 2-3 years.

1.3 Optical Coherence Tomography

1.3.1 Principle of OCT

Optical coherence tomography (OCT) uses interferometry to image ocular tissue⁽¹⁰¹⁾. Time-domain (TD-OCT) typically images with infrared light, that passes a partially reflective mirror anterior to the eye that splits light into two beams: One beam enters to the eye (sample arm), and the other beam is directed towards a moving reference mirror (reference arm)⁽¹⁰²⁾. A reflectivity profile is generated by quickly moving the reference arm mirror and simultaneously capturing the fringe pattern output. This profile is measured when the reference arm and reflective path distances are equal through the ocular tissue. Cross-sectional images are then produced from the series of separate profiles gathered by shifting the reference mirror while moving the beam over the eye. In contrast, spectral domain OCT (SD OCT) uses a stationary reference mirror, which, all other things being equal, provides better resolution⁽⁵⁶⁾ and either separates the interference into spectral components or uses a spectrally swept source. In spectral imaging, spectral (frequency) information, such as the Doppler shift, is collected at every location in an image plane. SD-OCT is able to extract spectral information by distributing different optical frequencies onto a detector. Fourier domain refers to the analysis of signals with respect to frequency, rather than time. In Fourier domain OCT, two configurations exist: Spectral domain OCT (SD-OCT), which utilizes a spectrometer; or swept-source OCT (SS-OCT), which uses a laser source⁽¹⁰³⁾. In SD-OCT, the spectrum is dispersed onto an array detector after travelling through a diffraction grating. In SS-OCT, a narrow band laser is swept across a broad spectrum, encoding the spectrum as a function of time. The swept source is superior to the spectral domain as it does not lose sensitivity at greater imaging depths. Therefore, SS-OCT is preferred choice if greater imaging depths are desired. With OCT, axial resolutions of a few microns can be

attained^(32, 33, 37, 41, 47, 51). OCT is now commonly used in ophthalmology, where images of ocular tissue of patients with disease can be acquired with higher resolutions^(42,48). Wojtkowski et al⁽⁵⁴⁾ showed the first *in vivo* retinal spectral domain OCT images. Wojtkowski et al⁽⁵⁴⁾ state “ultrahigh-resolution OCT in ophthalmic imaging has yielded axial resolutions of 3 μm in the retina compared to 10 μm for standard resolution OCT”. In addition, Doppler technologies have now been shown to have the ability to image ocular blood flow^(44,45).

1.3.2 Comparison of Commercial OCT Devices

A comparison of commercial OCT devices is shown in Table 1.1. Multiple considerations must be made when choosing the right OCT device for a clinical setting⁽⁵⁷⁾. In optometric clinics where there are perhaps no trained operators in using OCT, acquiring images when technology is first introduced becomes difficult. For instance, the addition of a mouse instead of the conventional joystick may be more appropriate for people who are familiar with mouse control through the use of a personal computer. Moreover, the clinician might sometimes weigh cost considerations over quality of images attainable. In smaller clinics, the size of the device might also be an important concern. For example, Cirrus HD-OCT is a relatively portable and space-efficient device while the Spectralis offers many ancillary devices/attachments. OCTs have different displays for scan results and this may also influence a clinician’s decision about what OCT is appropriate for their clinic. Lastly, the analysis software available is also an important factor. For example, the RTVue-100 allows for volumetric analysis to be performed.

OCT devices use different segmentation software and this could be an important factor for clinicians who are focusing their studies on specific diseases. Optometrists must also pay attention to updates in their retinal blood flow analysis software. By keeping up to date with the

newest advancements in OCT software, clinics may be required to change training protocol for their optometrists in order to improve the accuracy of retinal measurements.

Device	Manufacturer	Axial Resolution	Scanning Speed	Ancillary Devices	Notable Features
Stratus OCT	Carl Zeiss Meditec	10 μm	400 A-scans/sec.	NA	Time domain detection Current gold standard Least costly option
3D-OCT 1000	Topcon	6 μm	20,000 A-scans/sec.	Color non-mydratric fundus camera	Automatic pinpoint registration Software smoothly integrates with IMAGENet
3D SD OCT	Bioptogen	5 μm , upgradeable	20,000 A-scans/sec.	Doppler processing system Small animal probe Pediatric probe Corneal probe	Dual-engine light source: 1,310 nm and 820 nm Suitable for clinical and biomedical research
Cirrus HD-OCT	Carl Zeiss Meditec	5 μm	27,000 A-scans/sec.	NA	Space-saving, single-unit design Mouse-operated set up Dedicated live iris CCD camera Dedicated SLD fundus camera Retinal vessel tracing registration
Copernicus HR	Optopol Technology	3 μm	52,000 A-scans/sec.	Anterior chamber module (5 μm) Doppler analysis module	Fastest scan speed and highest resolution in a commercial OCT
RTVue-100	Optovue	5 μm	26,000 A-scans/sec.	Anterior chamber attachment lens	Real-time scan acquisition Only device to image retina, glaucoma and anterior segment Wide number of scan protocols and analysis functions Retinal vessel tracing registration Oversampling of specific points to decrease speckle
Spectral OCT/SLO	Ophthalmic Technologies	8 μm	27,000 A-scans/sec.	Confocal SLO Microperimetry to assess structure versus function	Real-time point-to-point registration Fast registration via confocal SLO
Spectralis HRA+OCT	Heidelberg Engineering	7 μm	40,000 A-scans/sec.	HRA (FA+ICG) Confocal SLO	Six imaging modalities: SD OCT, FA, ICG, fundus autofluorescence, 'red free' and IR Confocal dual beam scanning system for retinal tracking and registration Automatic rescan Oversampling of specific points to decrease speckle

Table 1.1 Comparison of Commercial OCT Devices.

Reprinted from Review of Ophthalmology, OCT Units: Which One is Right for Me?;16(9):62, Copyright (2009), with permission from Jobson Medical Information LLC.

1.3.3 RTVue-100 Spectral Domain Optical Coherence Tomography

Several noninvasive techniques have been developed to quantify retinal blood flow (RBF) in humans. Previous techniques for measuring RBF have numerous limitations, such as being invasive, or are subjective, or are incapable of calculating blood flow since a surrogate parameter of flow is truly measured. The Canon Laser Blood Flowmeter, or CLBF, is the only device that

truly measures volumetric retinal blood flow, but is limited to relatively large vessels and a single measurement site. To overcome these limitations, a new instrument has been developed, known as RTVue-100 SD-OCT.

RTVue-100 SD-OCT employs 840nm infrared light as its light source. A double circular scan pattern with concentric radii is used for the estimation of RBF and is positioned at the optic nerve head⁽⁵⁸⁾. With this scan, the angle of incidence can be obtained and this can provide blood flow velocity in absolute terms. The Doppler shift produced by the reflected light from the moving blood cells is quantified by a photodetector and translated by calculation to quantify the RBF by combining blood velocity values and the morphological measurement of retinal vessel calibre size⁽⁵⁹⁾. Doppler SD-OCT provides a more comprehensive assessment of RBF because it permits better imaging of fine arterioles; it measures both blood velocity and vessel diameter for all retinal vessels simultaneously allowing quantification of total retinal blood flow from 3 supranasal and 3 infranasal scans; and it measures retinal blood flow several times within a cardiac cycle (four measurement per second), which gives total time of measurement at 2 seconds for totaling the flow value⁽⁵⁸⁾. Reichel et al⁽⁵⁷⁾ state “the RTVue-100 acquires images in real time, which is particularly useful in patients who are prone to inattention, fixation losses or blinking during scans”. The RTVue-100 also has a wide number of available scan protocols and thus allows for multiple methods of viewing and analyzing the retinal layers and optic nerve.

1.4 Anatomy of Retinal Blood Circulation

The transport of retinal substances is facilitated by the inner retina and choroidal circulatory system. A diagram of the anatomy of the ophthalmic artery with various branches of the external carotid artery has been shown in Figure 1.1.

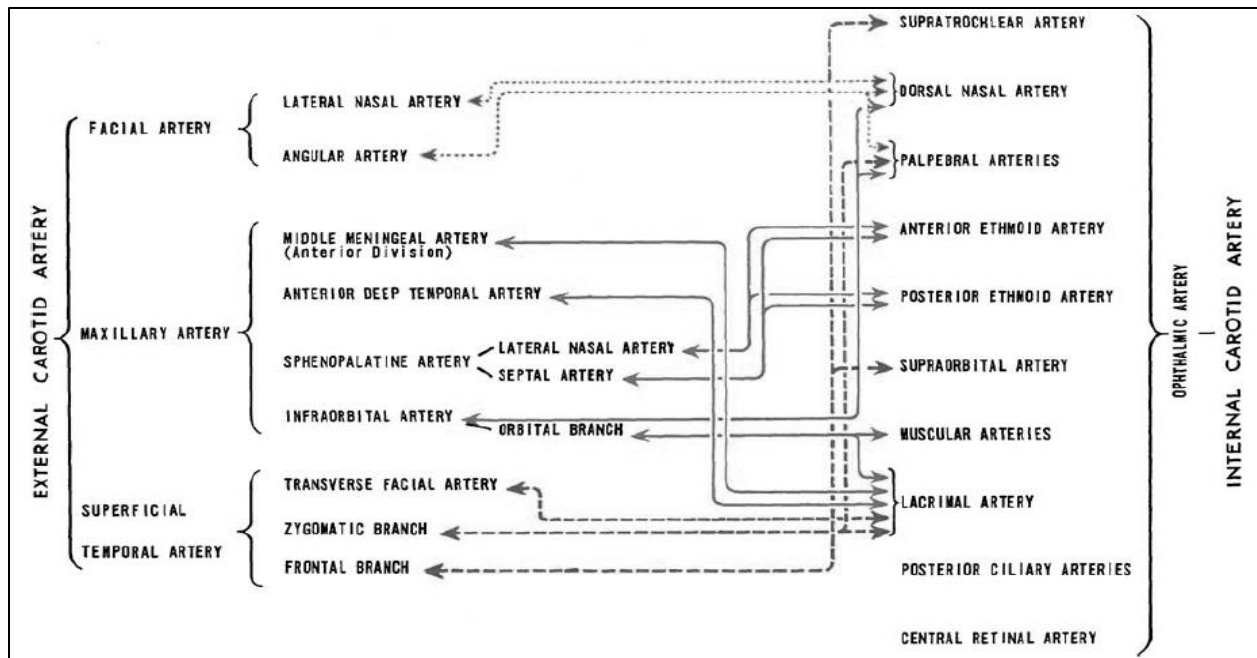


Figure 1.1 Diagram of anatomy of the ophthalmic artery.

Reprinted by permission from Macmillan Publishers Ltd: [EYE] (Hayreh SS. Orbital vascular anatomy), copyright (2006).

1.4.1 The Retinal Microvasculature

The retinal tissue is supplied by oxygen and nutrients by the inner and outer retinal vascular beds. The ophthalmic artery (OA) is the first branch of the internal carotid artery distal to the cavernous sinus⁽¹⁾. The OA eventually forms the central retinal artery (CRA) and is positioned underneath the globe. The inner and outer retina is supplied by the CRA and the choriocapillaris, respectively^(2, 3). In comparison to other arteries in vertebrates, arteriole branches of the CRA contain less smooth muscle and exhibit less involuntary control. The blood supply to the choroid comes from the ophthalmic artery. Posteriorly, these vessels divide into long posterior ciliary arteries and short posterior ciliary arteries. Choroidal blood supply circulates through the choriocapillaries and larger vessels of the choroid to drain into vortex veins. The vortex veins emerge posterior to the equator in quadrants. The superotemporal and

superonasal vortex veins drain into the superior ophthalmic vein. The inferonasal and inferotemporal vortex veins drain into the inferior ophthalmic vein. These vessels will eventually exit via the cavernous sinus.

1.4.2 Blood-Retinal Barrier

The blood-retinal barrier consists of the retinal vasculature and the retinal pigment epithelium (RPE). This barrier functions to ensure that specific substances do not enter the retina. A significant feature of the barrier is the presence of tight junctions⁽⁶⁾. These tight junctions are closely associated areas between two cells which aid in blocking the leakage of fluid. Within the outer retina, the RPE and Bruch's membrane (BM) create the *outer blood retinal barrier* (oBRB). The RPE limits retinal exposure to excessive light. The Bruch's membrane is a thin, acellular, five-layered extracellular matrix which assists in transfer between the retina and the choroid. There is supportive evidence that suggests that disruptions to the BM can lead to various eye-associated pathologies. Thus, characteristics of the BM are different in every individual and can distinctly affect the development of the visual environment.

1.5 Retinal Blood Flow Regulation

Blood flow through the retinal circulation is controlled by either the central nervous system (CNS) or by changes in the local environment⁽¹⁰⁰⁾. The retina has a mechanism that allows it to have approximately constant blood flow even in conditions of varying perfusion pressure⁽¹⁴⁾. This mechanism is known as *Autoregulation*. While most organs of the body exhibit some degree of autoregulation, it is not as evident in the ocular system, as opposed to the kidney, heart, or brain. Autoregulation in the retina can be caused by either a vascular response to a myogenic stimulus, metabolic changes, or in the presence of arterial gases.

1.5.1 Mechanisms of Autoregulation

Three mechanisms of retinal autoregulation exist, which include myogenic autoregulation, metabolic autoregulation, and autoregulation from arterial gases.

First, a myogenic response mechanism of pericyte cells in the retina exists which becomes activated during periods of high blood pressure⁽¹³⁾. Elevated blood flow can cause an increased level of blood pressure, which leads to involuntary vessel constriction. These vascular changes eventually allow for a stable blood flow to occur. Riva et al have assessed the efficacy of autoregulation to changes in blood pressure⁽⁹⁷⁾.

Second, metabolic autoregulation is another mechanism that alters blood flow to stabilize metabolic requirements of the organ⁽¹⁰⁰⁾. Retinal autoregulation is assisted by endothelium-derived factors^(4, 11). The vascular tone of the vessel may be altered by the release of certain metabolic substances. These endothelial specific derived relaxing factors (EDRF) are released by the endothelial cells and initiate a vasodilatory response within the vessel,⁽¹⁶⁾ and endothelial derived constricting factors (EDCF) provide a vasoconstricting response. Various studies have indicated that an important EDRF within the inner retinal vessels is nitric oxide (NO)⁽¹⁷⁻¹⁹⁾ and an important EDCF is endothelin-1 (ET-1)⁽⁴⁾.

Third, vascular change due to the presence of arterial gases can also elicit an autoregulatory response. The presence of oxygen (O₂) is essential in order for the retina to remain active in its functions and determines RBF⁽²²⁾. Ellsworth suggested that red blood cells respond to a low O₂ environment and the metabolic needs of the tissue by being able to augment blood flow and oxygen delivery wherever and whenever the need might arise⁽²³⁾. Another arterial gas which has an effect on retinal vessel tone is carbon dioxide (CO₂). Vasodilation of the retinal vessels can occur when there is an elevation in carbon dioxide arterial tension, also known as *hypercapnia*.

Previous studies that have investigated the normal retinal response to hypercapnia have found consistent increases in inner retinal blood flow⁽²⁴⁻²⁶⁾ and a relatively exaggerated effect on the cerebral vasculature⁽²⁷⁾. These studies are of particular interest because they investigate the potential use of RBF as an early indicator of stroke.

1.6 Blood Flow Dynamics

1.6.1 Ohm's Law

The underlying principles of physics that govern how current runs through a circuit are applicable to blood flow within a vessel. *Ohm's law* describes the relationship between flow and changes in pressure and resistance⁽⁸⁾.

$$Q = \frac{\Delta P}{R} \quad (1.1)$$

Flow (Q) is related to pressure change (ΔP) between the lengths of the tube and inversely related to the resistance (R). Pressure differences along the vessel segment results in blood moving from high pressure to low pressure regions. Resistance is dependent on various factors such as vessel size, vessel bed arrangement, physical properties of the blood and vasoactive substances acting upon the vasculature⁽¹⁰⁰⁾. As a general rule, Ohm's law states that higher resistance creates decreased blood flow through a vessel. All contemporary measurements for retinal blood flow (RBF) calculation assume a circular vessel profile. However, theoretical calculations will rarely provide exact values of blood flow as there will always be slight differences to practical values. Furthermore, due to the elasticity of each individual vessel, vessel profiles may not be circular and could assume other geometrical configurations, such as oval-shaped. As a consequence of this correction factor, an underestimation or overestimation of RBF could result.

1.6.2 Poiseuille's Law

Poiseuille's Law combines the study of liquid movement with the properties of a tube. This relationship is expressed as:

$$Q = \frac{\Delta P \pi r^4}{8 \eta L} \quad (1.2)$$

where the pressure gradient (ΔP), flow (Q), radius (r), viscosity (η) and dimensions (L) of the tube are associated. *Laminar flow* is the normal condition for blood flow throughout the circulatory system. It is characterized by concentric layers of blood moving in parallel down the length of a blood vessel⁽⁹⁶⁾. The result of this movement is that higher velocities occur in the middle, while lower velocities occur along the outer boundary. This law assumes that fluid behaves in a Newtonian manner, and flows freely without resistance. However, blood in the human cardiovascular system does not flow in a Newtonian fashion, as vessels are able to change size and contractions from the heart cause pulsatile blood flow.

1.6.3 Arterial Blood pressure

The pressure changes created throughout the cardiovascular system allows blood circulation to transport nutrients to and from cells in the body. A healthy range of maximum pressures during systole (ventricular contraction) and diastole (ventricular relaxation) is 120mmHg and 80mmHg, respectively⁽¹⁰⁴⁾. Blood pressure (BP) can be determined by the expression:

$$BP_{\text{mean}} = BP_{\text{dias}} + \frac{1}{3} (BP_{\text{sys}} - BP_{\text{dias}}) \quad (1.3)$$

where BP_{sys} is pressure measured during systole and BP_{dias} is pressure measured during diastole.

1.6.4 Inner and outer pressures of the eye

Aqueous humor is a fluid created by the ciliary body. It can follow either of two outflow pathways: 1) into the Schlemm canal known as the conventional pathway or 2) into the regions

between the sclera and choroid called the uveoscleral pathway⁽¹⁰⁴⁾. The resulting pressure from this transfer of aqueous humor is called the intraocular pressure (IOP). In goldmann applanation tonometry, the IOP is inferred from the force required to flatten a constant area of the cornea. In normal healthy individuals, IOP is in the range of 10-21 mmHg⁽¹⁰⁴⁾. The buildup of aqueous humor can cause an elevated IOP, and this can lead to optic neuropathy often clinically observed in the ocular disease known as glaucoma. The pressure of blood entering the eye, or ocular perfusion pressure (OPP), is influenced by BP and IOP in the formula:

$$\text{OPP} = \frac{2}{3} \text{BP}_{\text{mean}} - \text{IOP} \quad (1.4)$$

where BP_{mean} is the average blood pressure⁽⁹⁾.

1.7 Conclusion

Learning effects have been studied in the areas of surgical training, clinician trials, imaging techniques, and psychophysical testing. It has been shown that with training, operators are able to produce more accurate results. However, further studies are required to validate these results on newer technologies. One such example of a novel technology which requires validation is the RTVue-100 OCT. An understanding of the systemic and ocular blood pressures is important in order for the operator to accurately assess the patient's overall health status. The level of knowledge an operator has of the anatomical and physiological aspects of the retina could ultimately affect the overall assessment of learning effects associated with acquiring images with OCT.

Chapter 2 Rationale

2.1 Introduction

The role of an operator is demanding both in time and effort. High quality images can only be achieved through experience as OCT imaging using the RTVue-100 is highly sensitive and requires precise positioning and focus for accuracy. What represents a high quality image is in part a subjective evaluation and this evaluation may change over time. Operators may improve in their ability to acquire images as they become more familiar with SD-OCT technology. This improvement can be attributed to learning effects observed in both technology (i.e. joystick control) and the operator being able to allocate attention to specific task details such as looking for qualities that constitute a good image.

Although there are numerous studies published comparing the RTVue Doppler SD-OCT system to other optical instrumentations, there are no studies comparing the learning effects associated with acquiring Doppler SD-OCT images using this instrument. The reproducibility of ocular morphological measurements has been assessed, such as central corneal thickness (CCT),⁽⁷¹⁻⁷⁴⁾ retinal nerve fiber layer (RNFL) thickness,^(77, 79, 80) and optic disc measurements⁽⁷⁵⁾. However, there is insufficient information within the literature on whether operator experience impacts the outcome of the retinal blood flow measurements using Doppler SD-OCT.

2.2 Aims

The primary aim was to determine the presence of any learning effects with novice and experienced image acquisition. Image acquisition is a crucial stage in the validation of the RTVue-100 as extraneous factors *at the image acquisition stage* may influence the outcome of the RBF assessment. A comparison of the following parameters pertaining to image acquisition

was made: Total Acquisition Time (TAT), number of attempts to complete total scan protocol, and number of valid images.

2.3 Hypotheses

The hypotheses of this thesis were that total acquisition time (TAT) and number of attempts to complete total scan protocol will decrease, whereas the number of valid images of blood vessels will increase from novice to experienced sessions.

2.4 Conclusion

Overall, the aim of this thesis is to evaluate if there are improvements in the ability of operators to acquire ocular images through training. Understanding the influence of the level of experience on Doppler SD-OCT image acquisition is very valuable to determine if any apparent deviation of retinal blood flow (RBF) is truly significant or actually the product of extraneous influences such as learning effects. The image acquisition measurements will demonstrate significant differences between a novice and experienced operator.

Chapter 3

Materials and Methods

3.1 Introduction

The term “operator” has been used in this thesis to describe individuals who are being trained to operate OCT (i.e. OD students). The term “participant” has been used to describe individuals who are having their eye imaged. Operators and participants were not the same in this study. The sample size for participants and operators was calculated. Sample size determination is important in order to make inferences about a population from a sample. Inclusion and exclusion criteria were set up to select the participants and operators. Image acquisition and training protocol was kept the same for each operator in order to have an accurate comparison. Image acquisition parameters, including Total Acquisition Time (TAT), the number of attempts, and the number of valid scans, were measured and statistically analyzed to show significant differences between experience levels.

3.2 Sample Size determination

Using a pilot study (appendix), the average deviation in total acquisition time from novice to experienced level using Doppler SD-OCT on nine healthy participants was determined to be 6.92 ± 6.06 minutes. The standardized effect size ($= 6.92/6.06$) was computed to be 1.14 and the sample size (assuming $\alpha = 0.05$; power = 0.95) was 12 per group. Therefore, 12 operators were recruited for this study (12 “novice” operators transitioning to “experienced”).

3.3 Number of Participants estimation

Using G*Power statistical software⁽¹¹⁵⁾, I determined that nine participants will be used for the current study. Using an effect size of 1.14 and α error probability of 0.05, a power of 85 results with a total sample size of 9. This is to ensure that I achieve high statistical power and taking into

account for subject dropout considerations. A single eye of the participant will be chosen for the study.

3.4 Justification for the recruitment of Doctor of Optometry (OD) students

Fourth-year optometric students were chosen as test subjects for this study because they have been exposed to ocular health and disease, optics and visual sciences. Having also been exposed to numerous imaging modalities, such as fundus photography, these individuals also have the advantage of knowing what constitutes a good image. By year 4, these students have been exposed to techniques and behaviour training required for clinical practice. Furthermore, they have been exposed to patient contact and thus are quite comfortable when working with patients.

3.5 Definition of a novice and experienced operator

“novice” operator: An operator who has been newly trained by an “experienced” operator in image acquisition and has not acquired images on any participants using the RTVue SD-OCT.

“experienced” operator: An operator who has been newly trained by an “experienced” operator and has acquired images from at least 29 participants using the RTVue SD-OCT. With advice from Optovue Inc., it was suggested that completing 20 cases constitutes minimal experienced level.

3.6 Inclusion criteria for novice and experienced operator

Selected operators were from the University of Waterloo, School of Optometry and Vision Science. “Experienced” operators were selected from the pool of “Novice” operators.

Inclusion criteria for “novice” operator: A 4th year professional OD student with no previous experience using the RTVue SD-OCT.

Inclusion criteria for “experienced” operator: A 4th year professional OD student who has acquired images from at least 29 participants using the RTVue SD-OCT.

3.7 Imaged Participants

Selected participants were those who are healthy and free from systemic or ocular diseases. These participants were taken from a young population (age range: 20-30 years). Below are the criteria used to select participants in this study:

Inclusion criteria:

All volunteers passed a screening exam, which was conducted by a single optometrist. Each participant had a visual acuity of 6/6 or better. Participants had a refractive error within ± 6.00 Dioptres sphere (DS) and ± 2.00 Dioptres cylinder (DC). Corneal pachymetry was used to ensure participants have a central corneal thickness greater than 500 μm . Goldmann tonometry was used to ensure participants have an IOP of less than 21 mmHg as an IOP greater than this range indicates glaucoma.

Exclusion criteria:

Participant exclusions were made if the eye had significant media opacities likely to impair SD-OCT imaging. Participants were excluded if they had ocular surgery. The existence of any serious retinal or systemic disease that may affect RBF (i.e. diabetes, thyroid disorders, hypertension, etc.) also resulted in the exclusion of the participant. Smokers were excluded from the study.

The room temperature during the examination was maintained at 22 - 24 $^{\circ}$ C. Participants were asked to not drink caffeine products or consume red meat at minimum 4-12 hours before testing.

3.8 Procedures

3.8.1 Visits

Each operator was instructed to participate in two visits. At the initial visit, all operators acquired images from 9 participants using the RTVue SD-OCT. After the first visit, the novice operators

then acquired at least 20 additional cases to transition to “experienced” operator status. After gaining experience, these operators repeated image acquisition on the initial participants for the second visit.

3.8.2 Image Acquisition Protocol

The procedures for this study have been outlined in Figure 3.1. Assessment of best corrected logMAR visual acuity, blood pressure at rest, and intraocular pressure (IOP) were all done before dilating the eye with Tropicamide 0.5% (Alcon, Canada). IOP was assessed by a Goldmann applanation tonometer before and after readings were taken with the OCT.

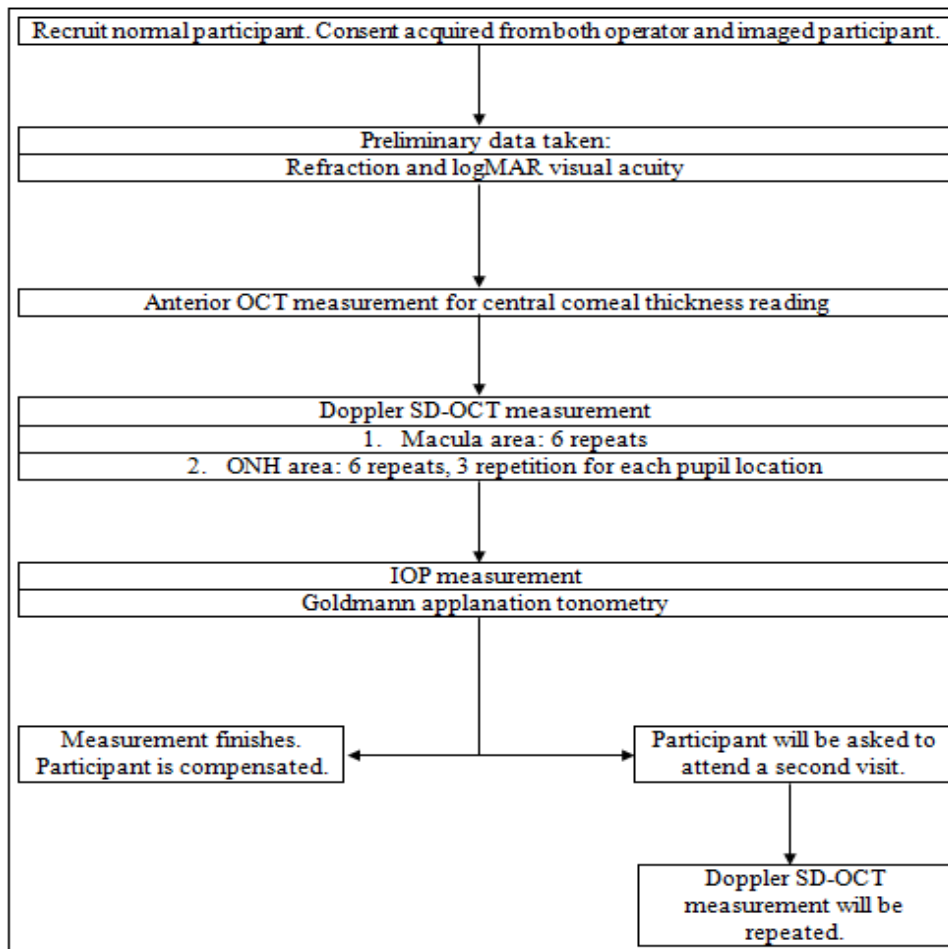


Figure 3.1 The detailed procedures for session.

Six repeats (for the new scan protocol; 3 repeat scans at each of 2 pupil positions) were acquired using the OCT at each visit. The operator first acquired 3 images at the supranasal pupil position and then acquired 3 images at the infranasal pupil position. These positions were chosen to provide variation in the imaging task and these are the positions most often used in total RBF assessment. A random eye of the participant was selected. The working distance between patients and the OCT was 22mm. The participant was instructed to put their chin on the slit-lamp and look at the blue target projected into the Doppler SD-OCT optical system (Figure 3.2). For the left eye, the fixation target was towards the right and for the right eye; the fixation target was towards the left to ensure a nasal position. The exposure power at pupil was $750\mu\text{W}$. This low value guaranteed no damage to imaged eyes being below the maximum permissible exposure dictated by the American National Standards Institute (ANSI) at this wavelength. Fundus photography was utilized to provide a documented confirmation of normality (Nidek Non-Mydriatic Auto Fundus Camera, Model AFC-230, 20 MP, Gamagori, Japan). Measurements were made while focused on the optic nerve head (ONH). The same image acquisition protocol was utilized for each visit.

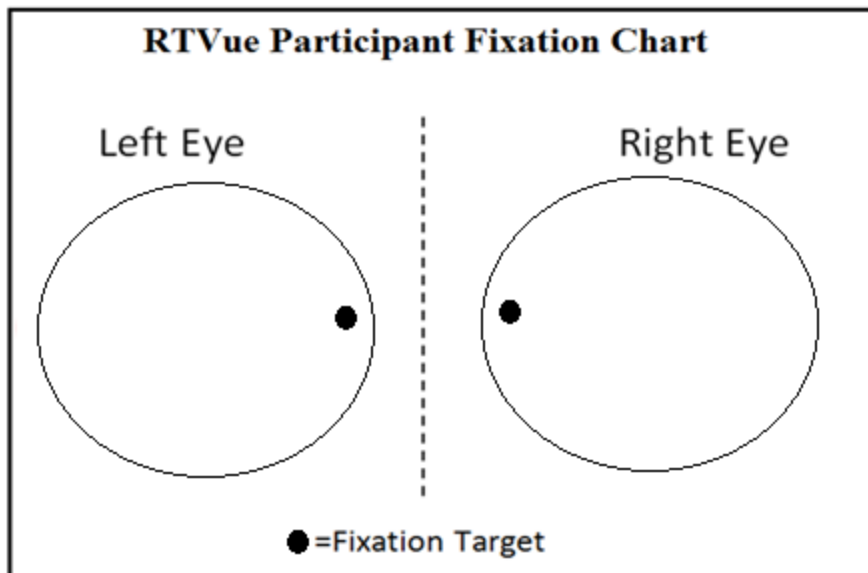


Figure 3.2 RTVue Participant Fixation Chart.

The RTVue-100 OCT provides an image-quality quantification known as the Signal Strength Index (SSI). Wang et al⁽⁹⁹⁾ define SSI as “a measure of the average signal strength across the scan; the higher the number, the better the quality”. Low SSI can result in poor image resolution, lack of retinal detail, and segmentation errors. The SSI can range from 0 (no signal) to 100 (very strong signal). The general guidelines from the manufacturer (Optovue) are as follows: SSI of <30 is a very poor quality scan that cannot be analyzed, SSI of 30-40 is a poor quality scan that can be analyzed but should be retaken to improve if possible, SSI of 40-50 is an adequate quality scan that can be analyzed but should be retaken to improve if possible, SSI of 50-60 is a good quality scan, SSI of >60 is a very good quality scan. SSI can be observed on the image quality check report after a scan is acquired (Figure 3.3). When a SSI of <30 is attained, the RTVue-100 OCT automatically commands the operator to re-take the respective poor-quality scan. However, if a SSI >30 is achieved, the image is accepted and the operator is instructed to continue to acquire the next scan.

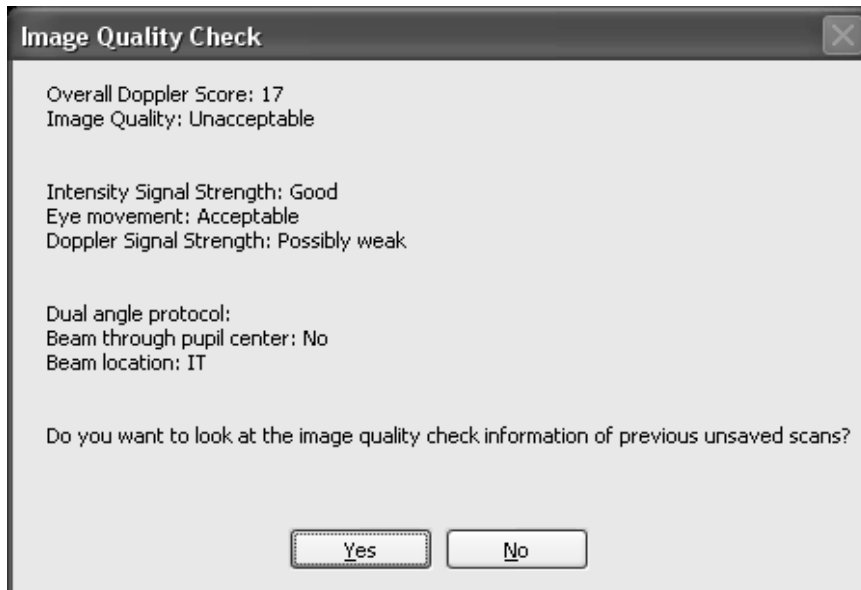


Figure 3.3 Image Quality Check. This report shows that the scan may have weak Doppler signal strength. In this scenario, the operator should move the beam to the edge of the pupil.

Reprinted by permission from Advanced Imaging for Glaucoma Study. AIGS Manual of Procedures 8.1.

3.8.3 Training Protocol

Operators were first shown two instructional videos (“How to take a scan?” and “How to take a 3D disk scan?”) produced by Optovue Inc. These videos taught operators on how to align participants and overviewed the scanning process with specific reference to focusing images.

After the videos, the training personnel (C.U.) then taught the operators about the start-up features, such as how to open the program, how to input participant information, and how to set up a scan protocol. I also taught the basic functionalities associated with the RTVue system, such as joystick maneuvering and the switches to move the instrument and chin rest (Figure 3.4).

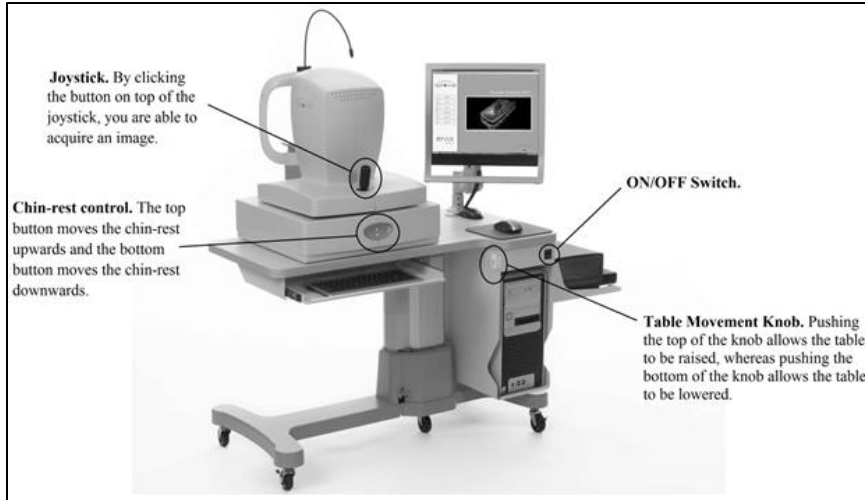


Figure 3.4 Operating controls for the RTVue-100.

The peak position of the curve pattern was shown to be adjusted by twisting the joystick (Figure 3.5). In order to acquire an image at the supranasal position, the operator twisted the joystick counter clockwise to move the curve's peak to the left. For the infranasal position, the operator twisted the joystick clockwise to move the curve's peak to the right. Once the height of the peak of the curve is positioned in the appropriate quadrant (upper-left for supranasal; upper-right for infranasal), this indicates that the beam is at the edge of the pupil and is in the correct location.

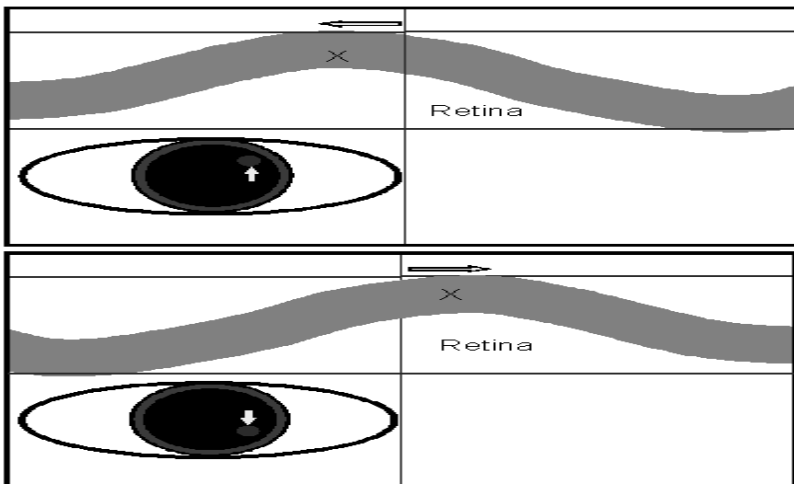


Figure 3.5 Supranasal Doppler Scan Position (*upper*). Infranasal Doppler Scan Position (*lower*).

Reprinted by permission from Advanced Imaging for Glaucoma Study. AIGS Manual of Procedures 8.1, Copyright (2012).

The training personnel (C.U.) then instructed each operator to follow and complete the RTVue training checklist (Figure 3.6).

<u>RTVue Acquisition Protocol ("Checklist"):</u>	<u>Training Personnel Protocol:</u>	
1. Open "RTVue" program located on desktop of computer. <input type="checkbox"/>	After viewing the instructional videos, the operator is then instructed to follow the RTVue checklist	
2. Click "New Patient" and enter patient information. <input type="checkbox"/>		
3. Click "Save/Examine". <input type="checkbox"/>		
4. Choose eye that will be examined (tick "OD" for right eye or tick "OS" for left eye) and enter # of scans for each. <input type="checkbox"/>	Instruct the operator to begin image acquisition and start electronic stopwatch	
5. Click "BF Study Protocol" under heading "Protocol". <input type="checkbox"/>		
6. Click "3D Disk" to begin acquisition. <input type="checkbox"/>		
7. Under the "advanced" tab, adjust the brightness. <input type="checkbox"/>		
8. Align the participant and instruct them to look at projected blue target. <input type="checkbox"/>		
9. Drag cross and focus it on the optic disc shown in the image. <input type="checkbox"/>	TAT	
10. Click "Auto All" to focus the image. <input type="checkbox"/>		
11. Click joystick when satisfied with image. Note: Images are acquired 2 seconds prior to clicking. <input type="checkbox"/>		
12. Save image by clicking  sign. If error, redo scan by clicking  sign. <input type="checkbox"/>		
13. Continue to "BloodFlow_DoubleRing" scan (repeat steps #6-11). <input type="checkbox"/>		
		Record an "attempt" for the operator
		Upon completion of the entire scan protocol, stop the electronic stopwatch

Figure 3.6 RTVue Training Checklist. Training personnel protocol has been included on the right side.

3.8.4 Quantitative Assessment of Image Acquisition Parameters

The total acquisition time (TAT) was measured by an electronic stopwatch ("start time" was when the training personnel (C.U.) instructed the operator to begin image acquisition and "end time" was when all images were successfully acquired).

While the operator was acquiring images, the training personnel (C.U.) recorded the number of attempts to complete total scan protocol (Note: An “attempt” was defined as when an operator had clicked to acquire an image).

The RTVue-100 software contains an algorithm that assesses if the scan acquired is “acceptable” or “unacceptable” based on numerous criteria, including image focus, resolution and signal strength. The Doppler OCT of Retinal Circulation (DOCTORC-Quality Check) software further evaluates the images acquired, paying specific attention to structural details, to check if the images can be analyzed for blood flow. Using the DOCTORC software on a separate computer, the number of valid scans was evaluated. This computer program was calibrated by Optovue Inc. prior to image quality assessment to ensure accurate results.

3.8.5 Statistical Analysis

After having established normality using Kolmogorov-Smirnov test, a paired samples t-test was performed to compare the effect of experience level on total acquisition time (TAT), the number of attempts, and the number of valid images. Within the study design, inter-operator relationships was evaluated (Figure 3.7). Analyses were completed with computer software (Statistica version 6; StatSoft, Tulsa, Oklahoma, USA).

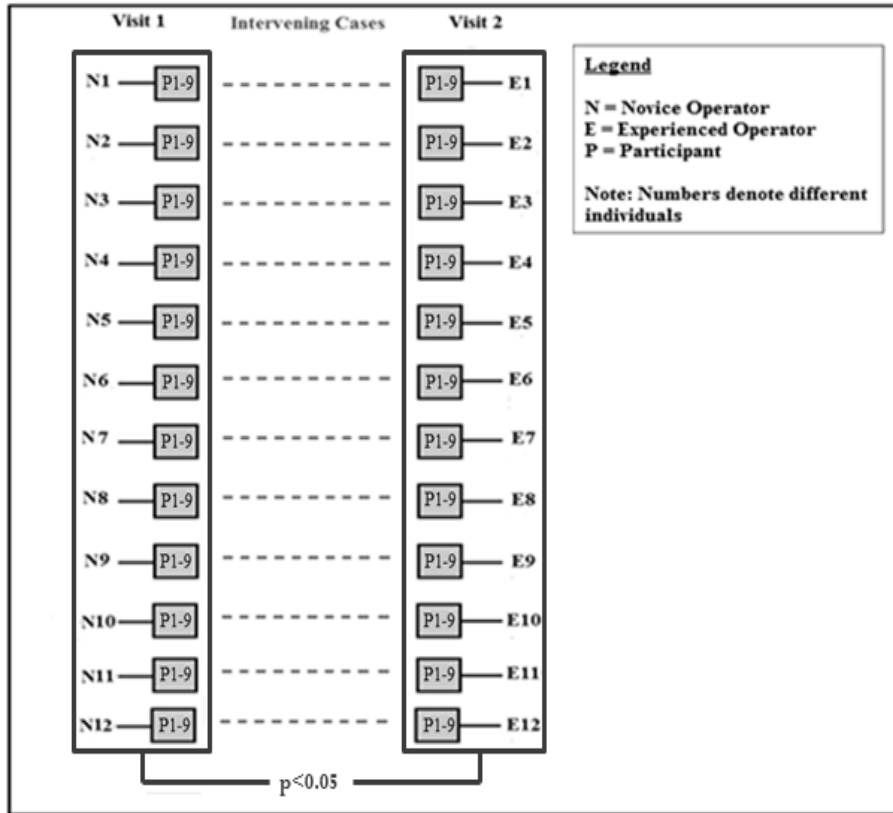


Figure 3.7 Study Design.

3.9 Conclusion

The sample size included twelve operators and nine participants. Doctor of Optometry (OD) students were selected for this study so a fair assessment of learning effects could be compared as each operator would have the same experience level at 2 visits. Inclusion and exclusion criteria were set up for participants in order to recruit individuals who were young and healthy. Inclusion and exclusion criteria were set up for operators in order to recruit individuals who were either “novice” or “experienced”.

Chapter 4 Results

4.1 Introduction

Participant characteristics were assessed to confirm healthy ranges of ocular and systemic parameters. The Kolmogorov-Smirnov test, or K-S test, was used to determine if the sampled data were from a normally distributed population. Image acquisition parameters, including Total Acquisition Time (TAT), the number of attempts, and the number of valid scans, were evaluated. Paired samples t-tests were used to show statistically significant differences between group means. Results were graphically presented by line graphs, box plots, scatter plots, and frequency distribution histograms.

4.2 Imaged participant characteristics

Imaged participants' characteristics are shown in Table 4.1. The mean age of the 9 subjects was 25.7 ± 3.8 years (mean \pm standard deviation; ranging from 23 to 30 years). All patients were emmetropic. Patient refractive error (RE) would affect RNFL thickness profile measured by RTVue OCT⁽¹⁰⁸⁾. While inputting patient information, there is an input which requests for RE and this can allow the OCT device to adjust for the axial length. Overall, imaged participants exhibited ocular and systemic parameters within normal ranges.

Table 4.1 Imaged participant characteristics

Age (years)	25.7 \pm 3.8
Systolic blood pressure (mmHg)	119.7 \pm 8.5
Diastolic blood pressure (mmHg)	74.0 \pm 14.2
Mean Arterial Pressure (mmHg)	89.2 \pm 12.3
Intraocular Pressure (mmHg)	15 \pm 2.6
Ocular Perfusion Pressure (mmHg)	44.5 \pm 5.6
Best-corrected visual acuity (<u>LogMAR</u>)	0 \pm 0.3
	<u>Snellen equivalent</u> ~20/20

Data are presented as means \pm s.d. ($n=3$).

4.3 Tests for Normality of Data

Figure 4.1 shows a frequency distribution histogram of the difference in total acquisition times from novice to experienced session. Although visually this graph does not appear to indicate normal distribution, the Kolmogorov-Smirnov (K-S) test for normality provided a K-S statistic $D=0.83$; $p=0.62$. Since the p-value is greater than the chosen alpha level (0.05), I can accept the null hypothesis that the data come from a normally distributed population. Hence, I can use paired samples t-test, which assumes normal distribution, to test my particular predictions.

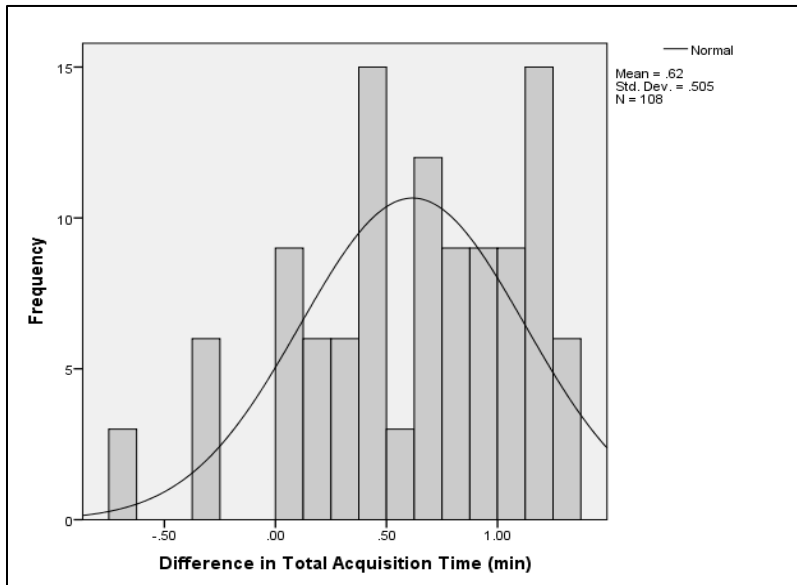


Figure 4.1 Histogram of Difference in Total Acquisition Time with Normal Distribution Curve.

4.4 Image Acquisition Parameters

4.4.1 Total Acquisition Time (TAT)

The group mean TAT, or the average TAT value from the 12 operators, was found to be 13.00 ± 6.3 minutes for the novice session, and for the experienced session it was 6.08 ± 1.93 minutes.

The difference in the TAT for the novice operators and experienced operators was statistically significant ($t(107)=11.87$, $p<0.001$). Figure 4.2 displays a line graph of the average total acquisition time (TAT) as a function of visit for each operator. A decline trend in the mean TAT

values can be observed from novice to experienced level. Figure 4.3 exhibits a box plot of the TAT as a function of visit. There was a greater median TAT value when the operators were novice (*Median* = 10.57 minutes) as compared to when the operators were experienced (*Median* = 5.89 minutes). Greater variability in TAT values can be observed in the novice session in comparison to the experienced session based on box size. The median line on the lower end of the box in the novice session indicates positively skewed data, whereby majority of the novice operators are achieving higher TAT values. However, the novice operators TAT values seem to become normalized relative to the experienced session. The scatter plot of the difference in TAT and the TAT at the novice session (Figure 4.4) shows a relatively strong correlation where the estimated R^2 was found to be 0.92. The strong experience effect observed in TAT suggests that those operators who had higher TAT values in the novice session tended to have the greatest reduction in TAT values in the experienced session. In contrast, operators who had lower TAT values in the novice session tended to have less reduction in TAT values in the experienced session. Figure 4.5 shows a frequency distribution histogram for TAT by the novice and experienced operators. It can be observed that no experienced operator took greater than 15 minutes to complete the entire scan protocol, whereas novice operators can be seen taking up to 30 minutes to complete this task. Figure 4.6 shows a frequency distribution histogram for the difference in TAT by the novice and experienced operators. An exponential decline trend, with relatively strong correlation ($R^2=0.93$), in the frequency can be observed with increasing difference in TAT. The majority of the difference in TAT was in 0-3 minutes, and the differences seem to plateau after this range. Overall, these results indicate that for more operators the changes in TAT were less.

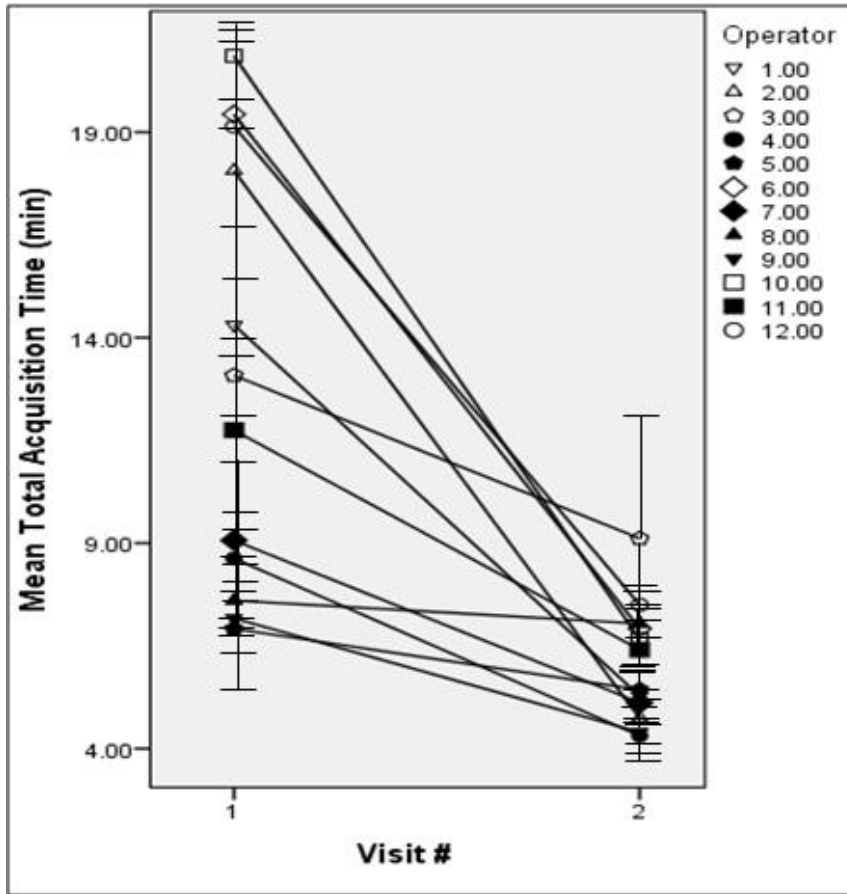


Figure 4.2 Line graph of the average Total Acquisition Time for each individual operator as a function of visit, where visits 1 and 2 represent the novice and experienced sessions, respectively.

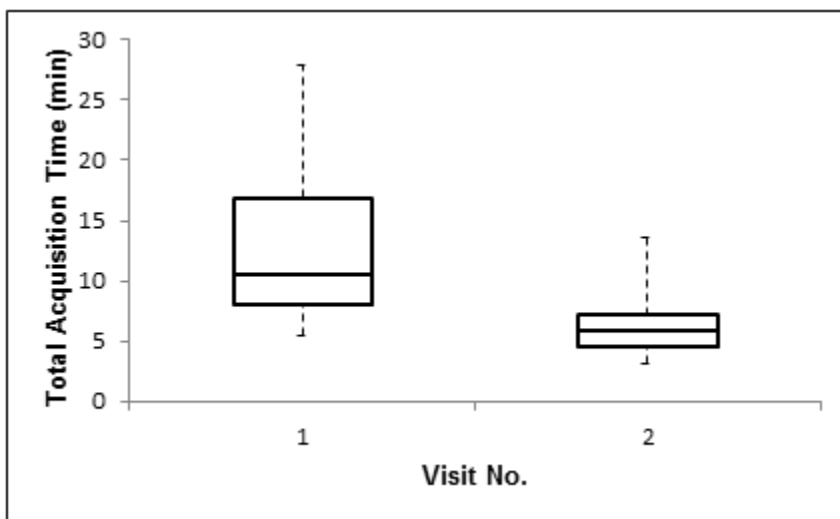


Figure 4.3 Box plot of Total Acquisition Time for each individual operator as a function of visit, where visits 1 and 2 represent the novice and experienced sessions, respectively.

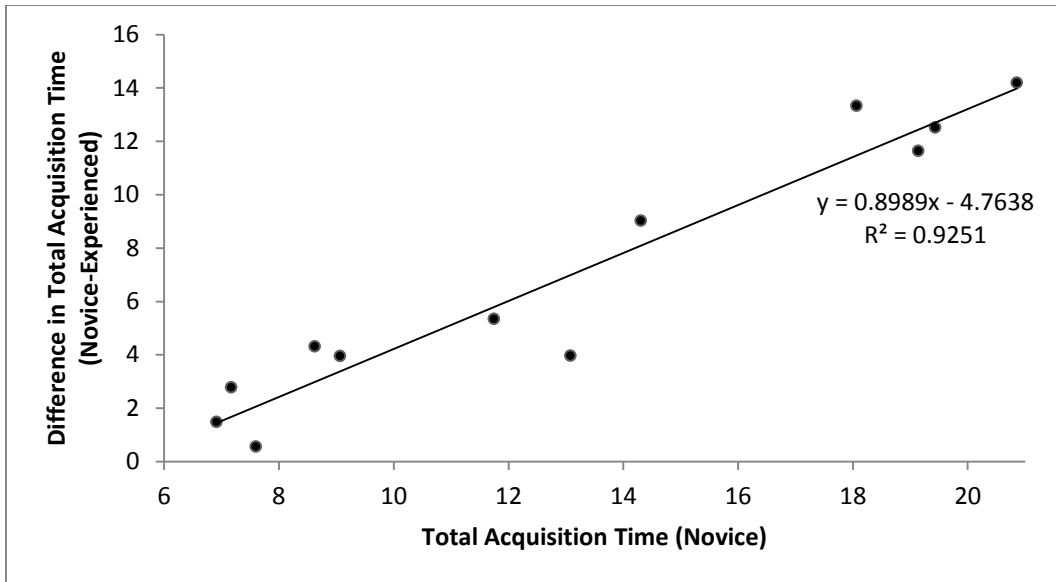


Figure 4.4 Scatter plot (with linear trend line) of the difference in Total Acquisition Time as a function of the Total Acquisition Time (Novice). The difference between two values was calculated as Novice minus Experienced value.

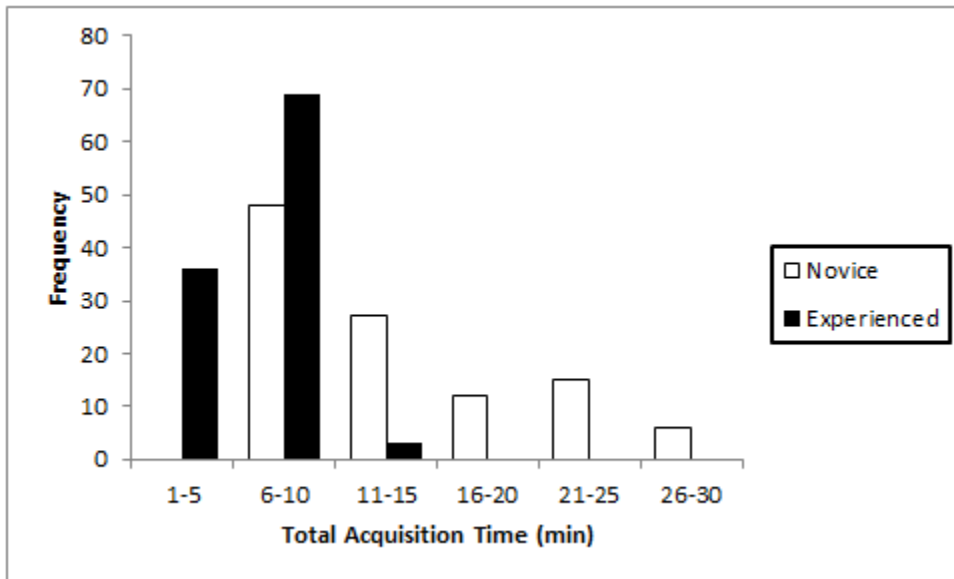


Figure 4.5 Frequency distribution histogram for Total Acquisition Time.

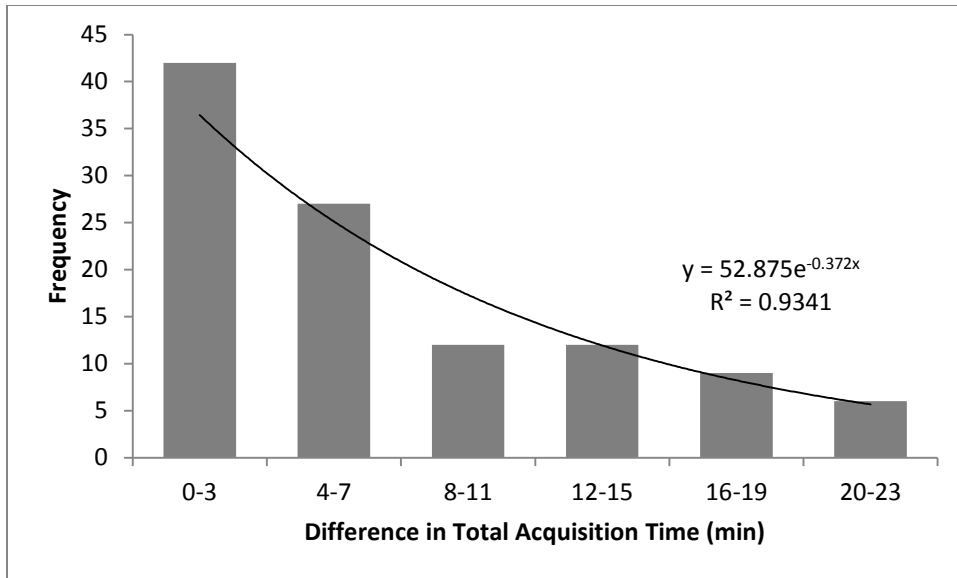


Figure 4.6 Frequency distribution histogram (fitted using exponential trend line) for the difference in Total Acquisition Time. The difference between two values was calculated as Novice minus Experienced value.

4.4.2 Number of Attempts

The group mean number of attempts, or the average number of attempts value from the 12 operators, required to acquire 6 scans was found to be 7.56 ± 1.87 attempts, and for the experienced session it was 6.19 ± 0.52 attempts. The difference in the total number of attempts required to acquire 6 scans for the novice operators and experienced operators was statistically significant ($t(107)=7.77$, $p<0.001$). Figure 4.7 displays a line graph of the average number of attempts as a function of visit for each operator. A decline trend in the mean number of attempts can be observed from novice to experienced level. The scatter plot of the change in the number of attempts and the number of attempts at the novice session (Figure 4.8) shows a relatively strong correlation where the estimated R^2 was found to be 0.93. The strong experience effect observed in the number of attempts suggests that those operators who had higher number of attempts in the novice session tended to have the greatest decline in the number of attempts in the experienced session. In comparison, operators who had lower number of attempts in the

novice session tended to have less reduction in the number of attempts in the experienced session. Figure 4.9 shows a frequency distribution histogram for number of attempts by the novice and experienced operators. It can be observed that no experienced operator took greater than 9 attempts to complete the entire scan protocol, whereas novice operators can be seen taking up to 15 attempts to complete this task. Figure 4.10 shows a frequency distribution histogram for the difference in number of attempts by the novice and experienced operators. The majority of the difference in number of attempts was in 0-2 attempts, and the differences seem to plateau after this range. Overall, these results indicate that for more operators the changes in TAT were less.

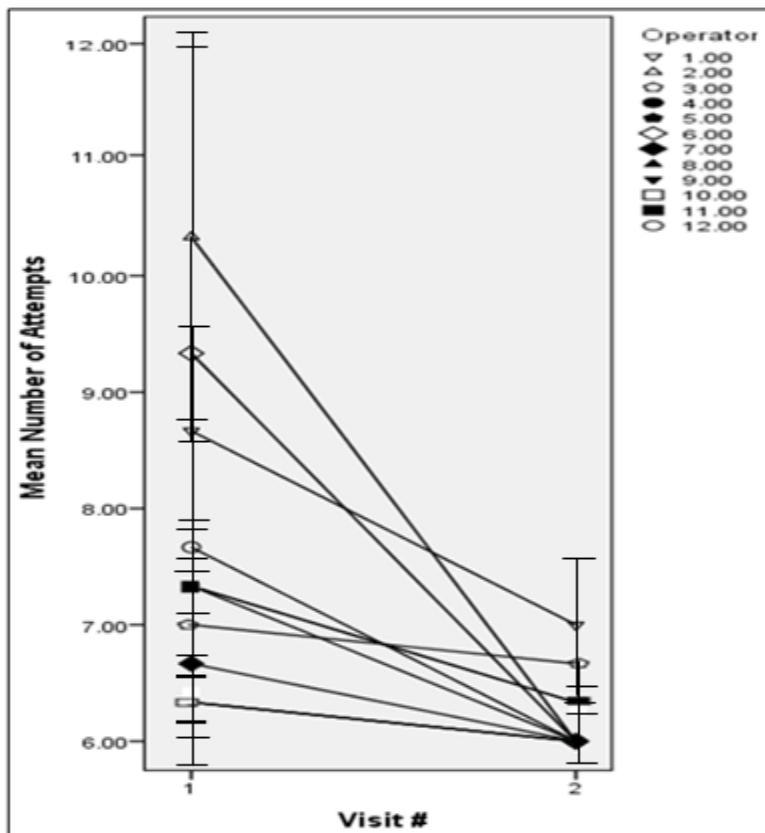


Figure 4.7 Line graph of the average number of attempts for each individual operator as a function of visit, where visits 1 and 2 represent the novice and experienced sessions, respectively.

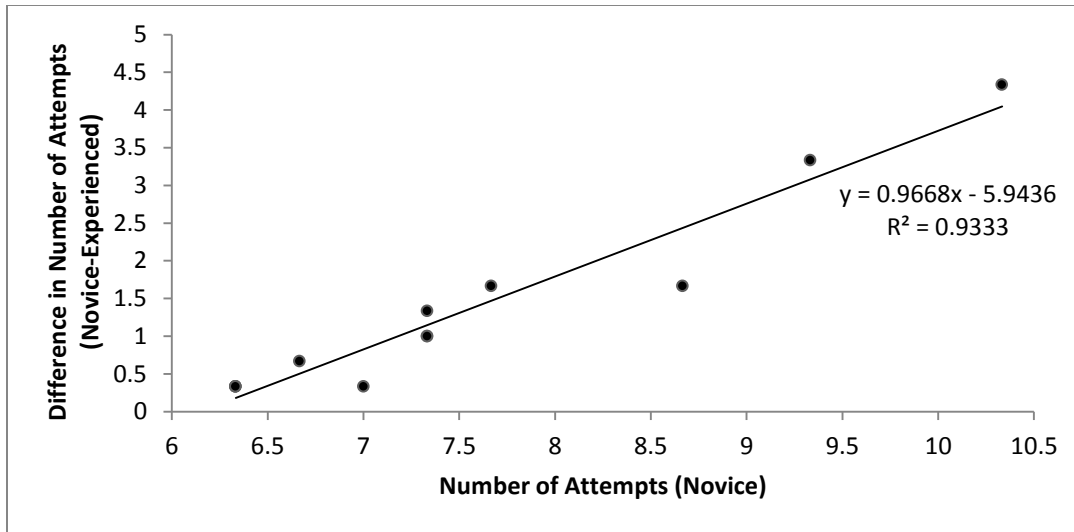


Figure 4.8 Scatter plot (with linear trend line) of the difference in Number of Attempts as a function of the Number of Attempts (Novice). The difference between two values was calculated as Novice minus Experienced value.

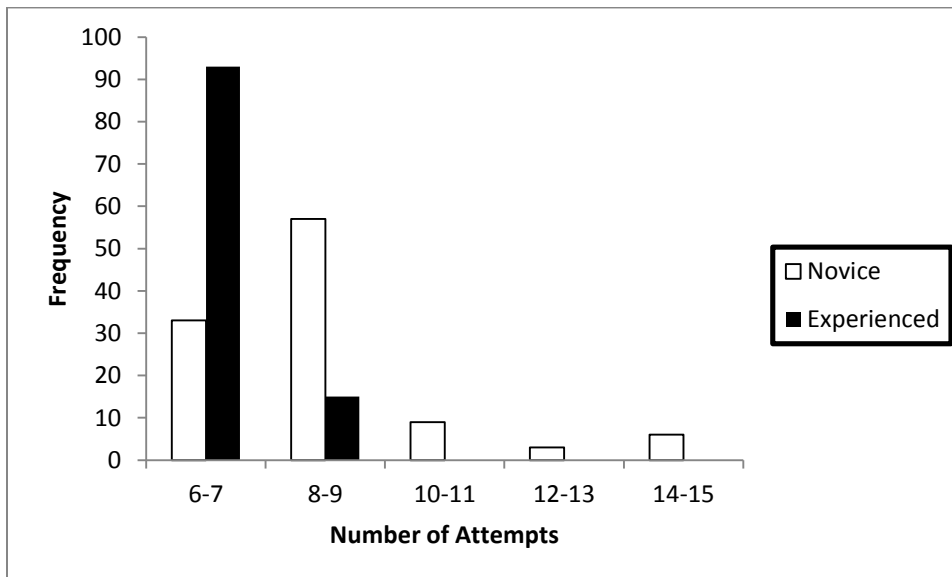


Figure 4.9 Frequency distribution histogram for Number of Attempts.

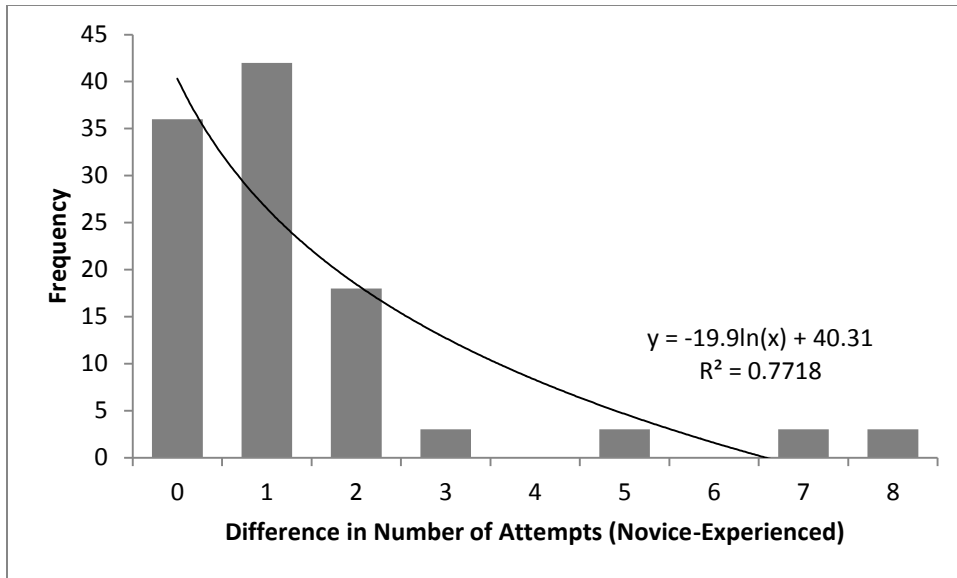


Figure 4.10 Frequency distribution histogram (fitted using logarithmic trend line) for the difference in Number of Attempts. The difference between two values was calculated as Novice minus Experienced value.

4.4.3 Number of Valid Images

Out of a total of 648 images, 354 (54.63%) and 453 (69.91%) were determined to be valid using the DOCTORC software (Centre for Ophthalmic Optics and Lasers, CA, USA) for the novice and experienced sessions, respectively. The group mean number of valid images, or the average number of valid images value from the 12 operators, was found to be 3.28 ± 1.94 images for the novice session, and for the experienced session it was 4.19 ± 1.62 images. The difference in the number of valid images for the novice operators and experienced operators was statistically significant ($t(107)=-4.14$; $p<0.001$). Figure 4.11 displays a line graph of the average number of valid images as a function of visit for each operator. Although an upwards trend in the mean number of valid images can be observed from novice to experienced level for most operators, there were three operators who had collected lower quality images. Figure 4.12 shows a frequency distribution histogram for the number of valid images by the novice and experienced operators. It can be observed that majority of the experienced operators were achieving 5-6 valid

images, whereas there is a whole spectrum of range from 0-6 valid images for the novice operators. Figure 4.13 shows a frequency distribution histogram for the difference in number of valid images by the novice and experienced operators. It can be observed that majority of the operators either gained or lost a single valid image when going from novice to experienced level. Overall, more operators gained rather than lost in their difference in number of valid images.

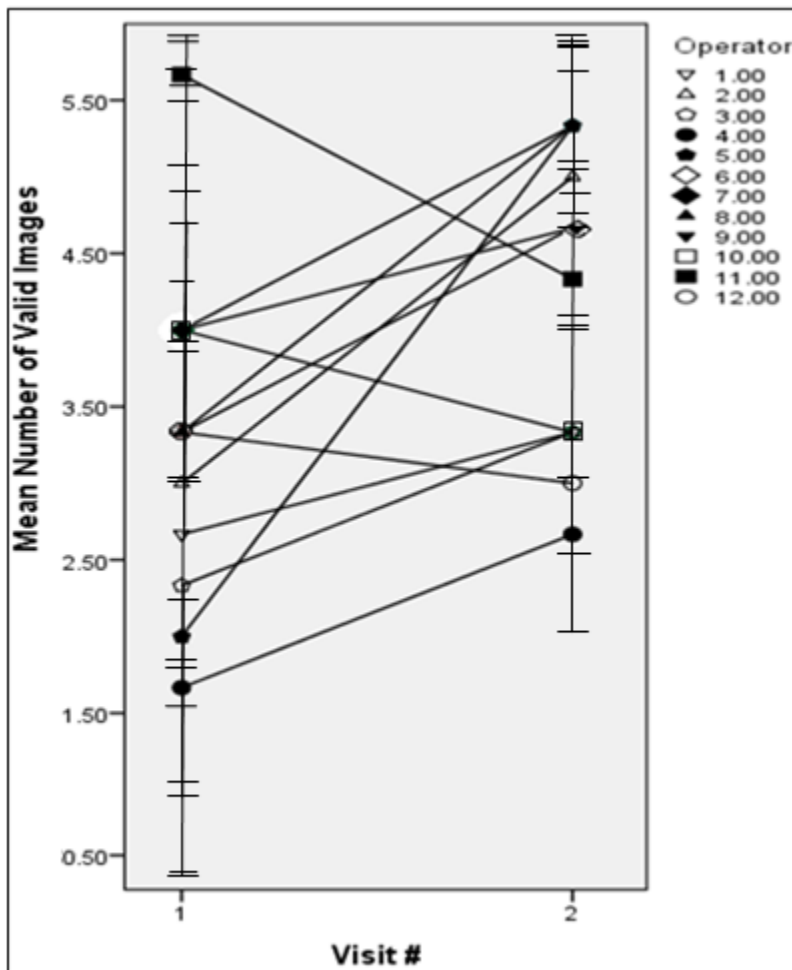


Figure 4.11 Line graph of the average number of valid images for each individual operator as a function of visit, where visits 1 and 2 represent the novice and experienced sessions, respectively.

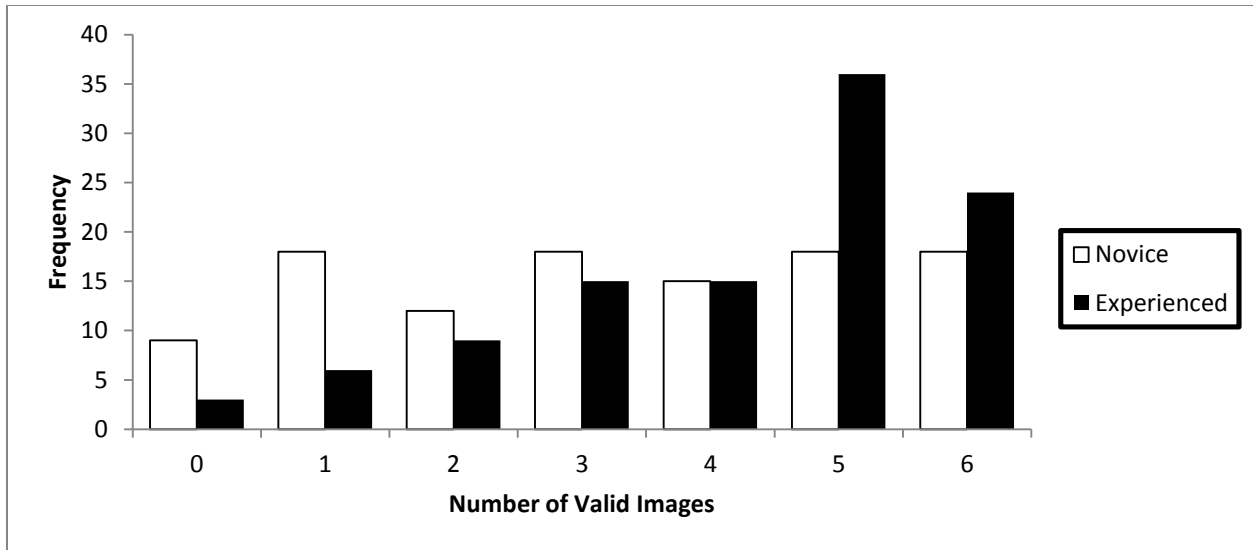


Figure 4.12 Frequency distribution histogram for Number of Valid Images.

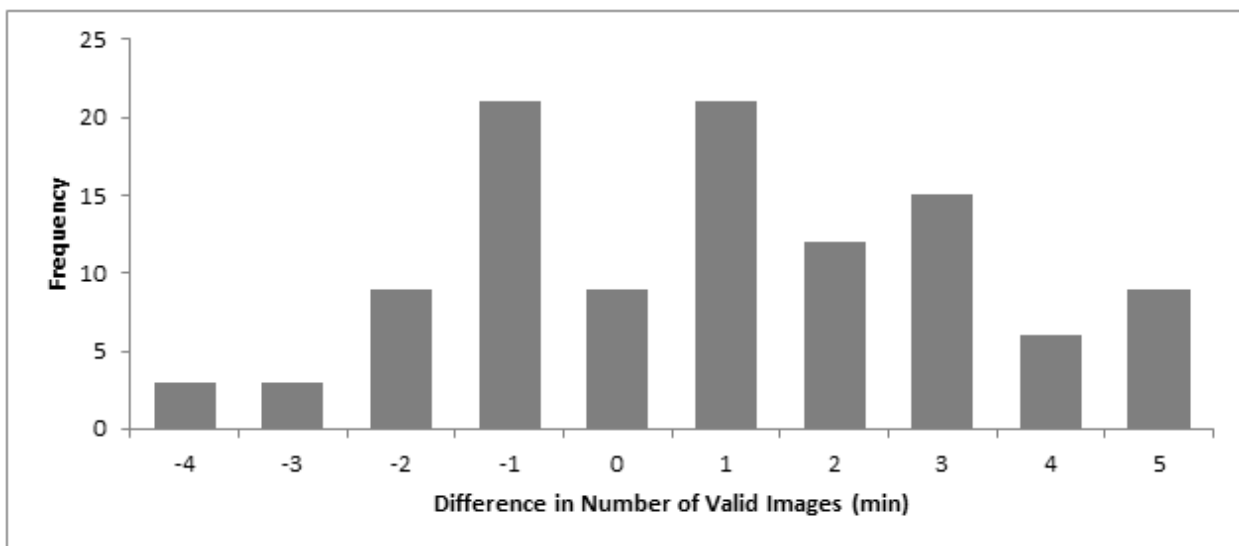


Figure 4.13 Frequency distribution histogram for the difference in Number of Valid Images. The difference between two values was calculated as Experienced minus Novice value.

4.4.4 Relationship between image acquisition parameters

Investigating the relationship between the image acquisition parameters may elucidate further information about the learning effects associated with image acquisition. The average speed of taking a single image was found to be 1.75 ± 0.86 minutes/attempts for the novice session, and for the experienced session it was 0.99 ± 0.32 minutes/attempts. The difference in the ratio of

TAT and number of attempts for the novice operators and experienced operators was statistically significant ($t(107)=9.97$; $p<0.001$). The degrees of freedom have been calculated based on 12 operators imaging 9 participants $[(12 \times 9) - 1 = 107]$. The relationship between TAT and the number of attempts resulted in a downwards trend (Figure 4.14), which could suggest that the experienced operators were indeed getting faster per image. It is important to note that these results reflect operators who have no prior experience using OCT. An individual who is experienced in OCT, regardless of having ever used RTVue-100, would be at an advantage and might be expected to show less of a learning effect with faster image acquisition within the early training process.

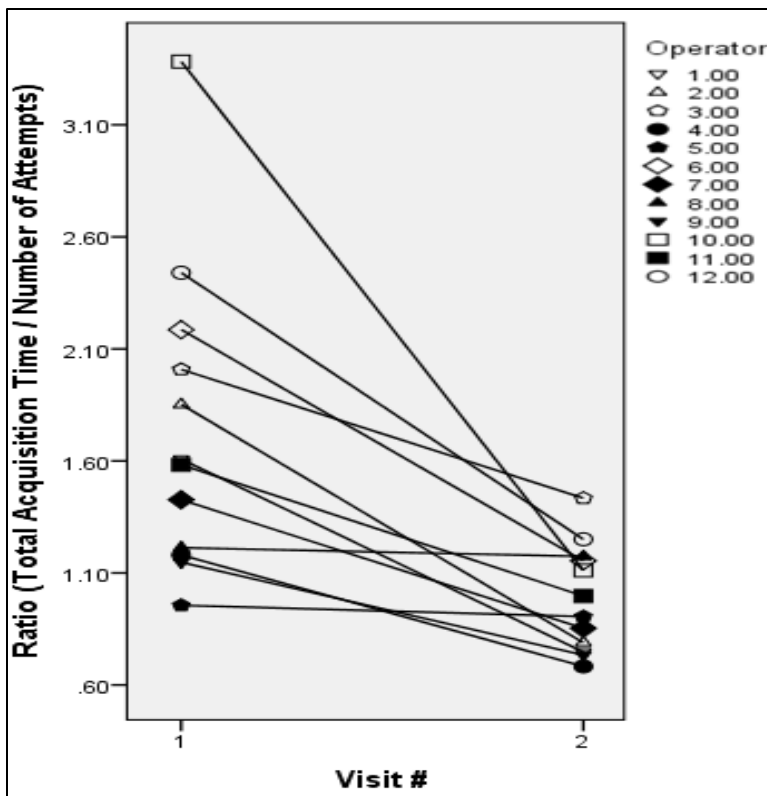


Figure 4.14 Line graph of the ratio of Total Acquisition Time and Number of Attempts as a function of visit, where visits 1 and 2 represent the novice and experienced sessions, respectively.

Based on Wang et al (2009), the amount of time it takes to acquire 6 scans (i.e. time from clicking the button to capturing the image) using the RTVue-100 can be estimated to be 3 seconds or 0.05 minutes. Hence, it takes approximately 0.5 seconds per scan or 0.0083 minutes. Assuming that operators took an equal amount of time per acquisition ($TAT/6 = 0.0083$ minutes), the group mean time to align a subject and focus a single image was found to be 2.16 ± 1.06 minutes for the novice session, and for the experienced session it was 1.00 ± 0.32 minutes. The group mean time to align a subject and focus a single image for the novice operators and experienced operators was statistically significant ($t(107)=11.85$; $p<0.001$). Hence, a decrease in the average time to align a subject and focus a single image was observed from the novice to experienced session (Figure 4.15). Less variability around this mean for the experienced group was also observed.

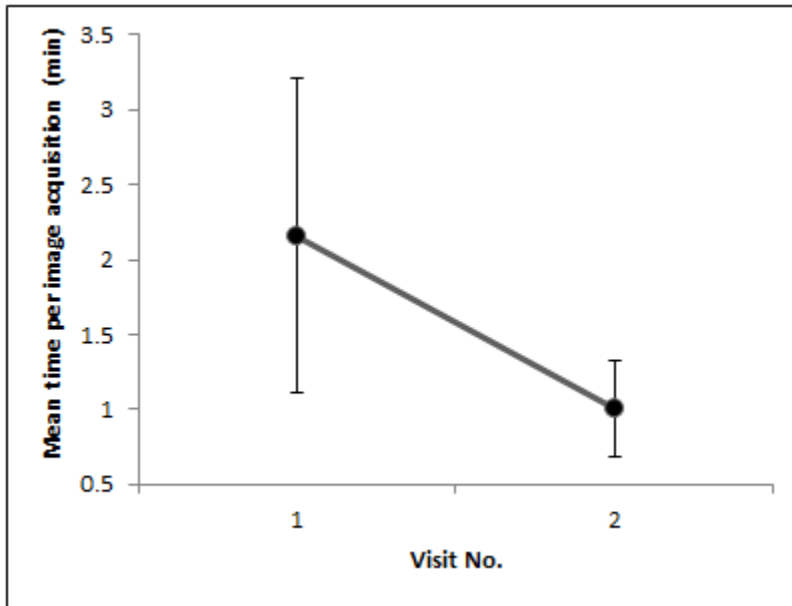


Figure 4.15 Line graph of the average time (with error bars) to align a subject and focus a single image as a function of visit, where visits 1 and 2 represent the novice and experienced sessions, respectively.

4.5 Conclusion

Table 4.2 outlines the differences in image acquisition parameters by experience level. For all parameters, there were significant differences ($p < 0.001$) in the means and standard deviations when comparing novice and experienced operators. Mean values for total acquisition time (TAT) and the number of attempts decreased, whereas the mean number of valid images increased from novice to experienced level. For each parameter, there was less variability around the experienced mean value compared to the novice mean value.

Image Acquisition Parameter	Experience Level	
	Novice	Experienced
Total Acquisition Time (min)		
Mean	13.00	6.08
±SD	±6.30	±1.93
p-value	p<0.001	
Number of Attempts		
Mean	7.56	6.19
±SD	±1.87	±0.52
p-value	p<0.001	
Number of Valid Images (DOCTORC)		
Mean	3.28	4.19
±SD	±1.94	±1.62
p-value	p<0.001	

Table 4.2. Differences in Image Acquisition Parameters by Experience Level. Group mean ± SD values for the image acquisition parameters at novice and experienced sessions.

Chapter 5

General Discussion

The findings from this study confirm that there are learning effects observed within the image acquisition process using the RTVue-100. These results propose that the experience level of the operator has a statistically significant effect on the total acquisition time (TAT), number of attempts, and number of valid images. The effect of experience level on the image acquisition parameters suggests that through training operators can acquire images in significantly less time, with less number of attempts to complete the entire scan protocol, and with greater number of valid images.

Although all operators had significant differences in their image acquisition parameter values when moving from novice to experienced level, the majority of these differences were small. With respect to the number of valid images, there were three operators who had collected lower quality images (Figure 4.11), which may suggest that the learning curve is different in each operator and that some may require more training than others in order to improve in their number of valid images. One study⁽¹¹²⁾ states that there may be a limit to the amount of improvement achieved through practice. It is possible that if an operator does not show training effects, perhaps their thresholds are already as low as they can be for that individual. Confounding variables involved in the image acquisition process were not measured. For example, an operator who is bored or careless would have an overall poor performance. The signal strength index (SSI) was also not measured as there is uncertainty about the accuracy of this parameter. SSI values of 0-30 cannot be used because these poorer (more noisy) images would not be of diagnostic value. There are no studies investigating the relationship between SSI and examiner's experience in RTVue-100. One study indicated significantly larger macular and optic nerve head OCT measurements were obtained with increasing SSI measurements, although differences were

small and were of questionable clinical importance⁽¹⁰⁵⁾. Comparing the Cirrus and Stratus OCTs, Moreno-Montanes⁽⁶²⁾ state “signal strength is independent of the examiner’s experience in Cirrus but not in Stratus. RNFL measurements obtained by both examiners were more reproducible with Cirrus than with Stratus OCT”. Mesiwala et al (2012) propose that determining the location of the disc margin by automatic and manual methods is in high correlation, and thus automatic software should replace manually conducted techniques in clinics as it can make OCT imaging more proficient. Another study⁽⁹²⁾ using Stratus OCT, indicated a high agreement of ONH measurements between automatic and manual assessment. The influence of learning effects on image acquisition may suggest the need for automatic software on the RTVue-100 to correct the variability among novice operators.

Along with the decline in TAT and the number of attempts, a decrease is observed in the average time to align a subject and focus a single image. Thus, operators were improving in their time values for completing all aspects of the image acquisition process. Intuitively, one would speculate that if an operator had greater number of attempts that this would lead to that individual having a higher Total Acquisition Time (TAT). However, looking at the ratio of TAT and number of attempts as a function of visit (Figure 4.14), the Number of Attempts has a slight impact on TAT as the graph follows a steeper decline trend from novice to experienced session than that observed when TAT was plotted as a function of visit (Figure 4.2). These findings could have significant clinical implications, because it infers that with adequate training inexperienced operators are able to reproduce higher quality RTVue-100 SD-OCT measurements. These results could be crucial to RBF assessment in ocular diseases that cause vision loss. There is a close link between reduced retinal blood flow and visual field loss in glaucoma that is largely independent of structural loss⁽¹⁰⁶⁾. Moreno-Montanes⁽⁶²⁾ et al state

“Good reproducibility and low variability are required in the RNFL thickness measurements using OCTs to evaluate glaucoma progression. Some factors are involved in this variability such as the collaboration of the patients, the experience of the examiner, the pupil dilation, and variations in the signal strength”. When using RTVue-100, patient experience and age does not impact reproducibility of peripapillary RNFL thickness⁽¹⁰⁹⁾. However, patient-related factors that could potentially influence the instrument’s signal-to-noise ratio include glaucoma severity and pupil size⁽¹⁰⁹⁾. The exact association between operator experience and image acquisition using SD-OCT is yet to be determined. More understanding of this association is crucial because in a practical setting it is difficult to run an entire scan protocol for extended periods of time using a single operator⁽⁶²⁾. To my knowledge, there are no published studies in Medline or ISI index comparing novice versus experienced image acquisition using the RTVue-100 SD-OCT. However, there is a preliminary study which has indicated that the use of automated machine learning classifiers in Stratus OCT image acquisition might be useful for enhancing the utility of this technology for detecting glaucomatous abnormality⁽¹⁰⁷⁾.

This study had certain limitations. The relatively small sample size should be considered when interpreting the results. However, the study sample provided 95% power according to the power computation. It is also important to note that the sampling in this study was very specific. The results cannot be generalized to all groups of students. For example, optometry students from another Canadian optometry school could be expected to have similar results. However, if students were sampled from a different discipline, such as social sciences, there may be less of an improvement as these students would have to first learn the basics of ocular anatomy in addition to how to operate an OCT. It is possible to train any individual to acquire images using OCT, however the amount of training required to achieve high quality images will vary among

different groups of individuals. One topic that remains to be explored is to determine whether image acquisition parameters influence RBF values using SD-OCT.

In summary, through experience operators can acquire higher quality images with the RTVue-100 SD-OCT in less time. Appropriate training programs should be developed to train clinicians in the use of the RTVue-100 to ensure efficient OCT image acquisition.

References

1. Hayreh SS. Orbital vascular anatomy *Eye (Lond)*. 2006;20(10):1130-1144.
2. Wangsa-Wirawan ND, Linsenmeier RA. Retinal oxygen: Fundamental and clinical aspects *Arch Ophthalmol*. 2003;121(4):547-557.
3. Yu DY, Cringle SJ. Oxygen distribution and consumption within the retina in vascularised and avascular retinas and in animal models of retinal disease *Prog Retin Eye Res*. 2001;20(2):175-208.
4. Pournaras CJ, Rungger-Brandle E, Riva CE, Hardarson SH, Stefansson E. Regulation of retinal blood flow in health and disease *Prog Retin Eye Res*. 2008;27(3):284-330.
5. Shakib M, Cunha-Vaz JG. Studies on the permeability of the blood-retinal barrier. IV. junctional complexes of the retinal vessels and their role in the permeability of the blood-retinal barrier *Exp Eye Res*. 1966;5(3):229-234.
6. Cunha-Vaz J. The blood-ocular barriers *Surv Ophthalmol*. 1979;23(5):279-296.
7. Booij JC, Baas DC, Beisekeeva J, Gorgels TG, Bergen AA. The dynamic nature of bruch's membrane *Prog Retin Eye Res*. 2010;29(1):1-18.
8. Berne, R. and Levy MN, ed. *Principals of Physiology*. 3rd ed. Michigan: Mosby Inc.; 2000.
9. Riva CE, Sinclair SH, Grunwald JE. Autoregulation of retinal circulation in response to decrease of perfusion pressure *Invest Ophthalmol Vis Sci*. 1981;21(1 Pt 1):34-38.
10. Dumskyj MJ, Eriksen JE, Dore CJ, Kohner EM. Autoregulation in the human retinal circulation: Assessment using isometric exercise, laser doppler velocimetry, and computer-assisted image analysis *Microvasc Res*. 1996;51(3):378-392.

11. Rassam SM, Patel V, Kohner EM. The effect of experimental hypertension on retinal vascular autoregulation in humans: A mechanism for the progression of diabetic retinopathy *Exp Physiol*. 1995;80(1):53-68.
12. Sinclair SH, Grunwald JE, Riva CE, Braunstein SN, Nichols CW, Schwartz SS. Retinal vascular autoregulation in diabetes mellitus *Ophthalmology*. 1982;89(7):748-750.
13. Delaey C, Van de Voorde J. Pressure-induced myogenic responses in isolated bovine retinal arteries *Invest Ophthalmol Vis Sci*. 2000;41(7):1871-1875.
14. Nagaoka T, Mori F, Yoshida A. Retinal artery response to acute systemic blood pressure increase during cold pressor test in humans *Invest Ophthalmol Vis Sci*. 2002;43(6):1941-1945.
15. Polito A, Polini G, Chiodini RG, Isola M, Soldano F, Bandello F. Effect of posture on the diurnal variation in clinically significant diabetic macular edema *Invest Ophthalmol Vis Sci*. 2007;48(7):3318-3323.
16. Robinson F, Riva CE, Grunwald JE, Petrig BL, Sinclair SH. Retinal blood flow autoregulation in response to an acute increase in blood pressure *Invest Ophthalmol Vis Sci*. 1986;27(5):722-726.
17. Delaey C, Boussery K, Van de Voorde J. A retinal-derived relaxing factor mediates the hypoxic vasodilation of retinal arteries *Invest Ophthalmol Vis Sci*. 2000;41(11):3555-3560.
18. Dorner GT, Garhofer G, Kiss B, et al. Nitric oxide regulates retinal vascular tone in humans *Am J Physiol Heart Circ Physiol*. 2003;285(2):H631-6.
19. Nagaoka T, Sakamoto T, Mori F, Sato E, Yoshida A. The effect of nitric oxide on retinal blood flow during hypoxia in cats *Invest Ophthalmol Vis Sci*. 2002;43(9):3037-3044.

20. Schmetterer L, Polak K. Role of nitric oxide in the control of ocular blood flow *Prog Retin Eye Res.* 2001;20(6):823-847.
21. Polak K, Luksch A, Frank B, Jandrasits K, Polska E, Schmetterer L. Regulation of human retinal blood flow by endothelin-1 *Exp Eye Res.* 2003;76(5):633-640.
22. Granger HJ, Shepherd AP, Jr. Intrinsic microvascular control of tissue oxygen delivery *Microvasc Res.* 1973;5(1):49-72.
23. Ellsworth ML. The red blood cell as an oxygen sensor: What is the evidence? *Acta Physiol Scand.* 2000;168(4):551-559.
24. Dorner GT, Garhofer G, Zawinka C, Kiss B, Schmetterer L. Response of retinal blood flow to CO₂-breathing in humans *Eur J Ophthalmol.* 2002;12(6):459-466.
25. Venkataraman ST, Hudson C, Fisher JA, Flanagan JG. Novel methodology to comprehensively assess retinal arteriolar vascular reactivity to hypercapnia *Microvasc Res.* 2006;72(3):101-107.
26. Venkataraman ST, Hudson C, Fisher JA, Flanagan JG. The impact of hypercapnia on retinal capillary blood flow assessed by scanning laser doppler flowmetry *Microvasc Res.* 2005;69(3):149-155.
27. Venkataraman ST, Hudson C, Fisher JA, Rodrigues L, Mardimae A, Flanagan JG. Retinal arteriolar and capillary vascular reactivity in response to isoxic hypercapnia *Exp Eye Res.* 2008;87(6):535-542.
28. McMillan DE, Utterback NG, Stocki J. Low shear rate blood viscosity in diabetes *Biorheology.* 1980;17(4):355-362.

29. Ernst E, Matrai A. Altered red and white blood cell rheology in type II diabetes *Diabetes*. 1986;35(12):1412-1415.
30. MacRury SM, Lowe GD. Blood rheology in diabetes mellitus *Diabet Med*. 1990;7(4):285-291.
31. Lowe GD, Ghafour IM, Belch JJ, Forbes CD, Foulds WS, MacCuish AC. Increased blood viscosity in diabetic proliferative retinopathy *Diabetes Res*. 1986;3(2):67-70.
32. Bizheva K, Povazay B, Hermann B, et al. Compact, broad-bandwidth fiber laser for sub-2-microm axial resolution optical coherence tomography in the 1300-nm wavelength region *Opt Lett*. 2003;28(9):707-709.
33. Bourquin S, Aguirre A, Hartl I, et al. Ultrahigh resolution real time OCT imaging using a compact femtosecond Nd:Glass laser and nonlinear fiber *Opt Express*. 2003;11(24):3290-3297.
34. Chinn SR, Swanson EA, Fujimoto JG. Optical coherence tomography using a frequency-tunable optical source *Opt Lett*. 1997;22(5):340-342.
35. Choma M, Sarunic M, Yang C, Izatt J. Sensitivity advantage of swept source and fourier domain optical coherence tomography *Opt Express*. 2003;11(18):2183-2189.
36. Drexler W, Morgner U, Ghanta RK, Kartner FX, Schuman JS, Fujimoto JG. Ultrahigh-resolution ophthalmic optical coherence tomography *Nat Med*. 2001;7(4):502-507.
37. Drexler W, Morgner U, Kartner FX, et al. In vivo ultrahigh-resolution optical coherence tomography *Opt Lett*. 1999;24(17):1221-1223.
38. Drexler W, Sattmann H, Hermann B, et al. Enhanced visualization of macular pathology with the use of ultrahigh-resolution optical coherence tomography *Arch Ophthalmol*. 2003;121(5):695-706.

39. Fujimoto JG. Optical coherence tomography for ultrahigh resolution in vivo imaging *Nat Biotechnol.* 2003;21(11):1361-1367.
40. Golubovic B, Bouma BE, Tearney GJ, Fujimoto JG. Optical frequency-domain reflectometry using rapid wavelength tuning of a Cr⁴⁺:Forsterite laser *Opt Lett.* 1997;22(22):1704-1706.
41. Hartl I, Li XD, Chudoba C, et al. Ultrahigh-resolution optical coherence tomography using continuum generation in an air-silica microstructure optical fiber *Opt Lett.* 2001;26(9):608-610.
42. Hee MR, Izatt JA, Swanson EA, et al. Optical coherence tomography of the human retina *Arch Ophthalmol.* 1995;113(3):325-332.
43. Huang D, Swanson EA, Lin CP, et al. Optical coherence tomography *Science.* 1991;254(5035):1178-1181.
44. Leitgeb R, Schmetterer L, Drexler W, Fercher A, Zawadzki R, Bajraszewski T. Real-time assessment of retinal blood flow with ultrafast acquisition by color doppler fourier domain optical coherence tomography *Opt Express.* 2003;11(23):3116-3121.
45. Leitgeb RA, Schmetterer L, Hitzenberger CK, et al. Real-time measurement of in vitro flow by fourier-domain color doppler optical coherence tomography *Opt Lett.* 2004;29(2):171-173.
46. Nassif N, Cense B, Park BH, et al. In vivo human retinal imaging by ultrahigh-speed spectral domain optical coherence tomography *Opt Lett.* 2004;29(5):480-482.
47. Povazay B, Bizheva K, Unterhuber A, et al. Submicrometer axial resolution optical coherence tomography *Opt Lett.* 2002;27(20):1800-1802.

48. Puliafito CA, Hee MR, Lin CP, et al. Imaging of macular diseases with optical coherence tomography *Ophthalmology*. 1995;102(2):217-229.
49. Smith LM, Dobson CC. Absolute displacement measurements using modulation of the spectrum of white light in a michelson interferometer *Appl Opt*. 1989;28(16):3339-3342.
50. Swanson EA, Huang D, Hee MR, Fujimoto JG, Lin CP, Puliafito CA. High-speed optical coherence domain reflectometry *Opt Lett*. 1992;17(2):151-153.
51. Wang Y, Zhao Y, Nelson JS, Chen Z, Windeler RS. Ultrahigh-resolution optical coherence tomography by broadband continuum generation from a photonic crystal fiber *Opt Lett*. 2003;28(3):182-184.
52. Wojtkowski M, Bajraszewski T, Gorczynska I, et al. Ophthalmic imaging by spectral optical coherence tomography *Am J Ophthalmol*. 2004;138(3):412-419.
53. Wojtkowski M, Bajraszewski T, Targowski P, Kowalczyk A. Real-time in vivo imaging by high-speed spectral optical coherence tomography *Opt Lett*. 2003;28(19):1745-1747.
54. Wojtkowski M, Srinivasan V, Ko T, Fujimoto J, Kowalczyk A, Duker J. Ultrahigh-resolution, high-speed, fourier domain optical coherence tomography and methods for dispersion compensation *Opt Express*. 2004;12(11):2404-2422.
55. Yun SH, Boudoux C, Tearney GJ, Bouma BE. High-speed wavelength-swept semiconductor laser with a polygon-scanner-based wavelength filter *Opt Lett*. 2003;28(20):1981-1983.
56. Al-latayfeh MM, Sun JK, Aiello LP. Ocular coherence tomography and diabetic eye disease *Semin Ophthalmol*. 2010;25(5-6):192-197.
57. Reichel E, Ho J, Duker JS. OCT Units: Which One is Right for Me? *Review of Ophthalmology*. 2009; 16(9): 62.

58. Wang Y, Lu A, et al. Measurement of total blood flow in the normal human retina using Doppler Fourier-domain optical coherence tomography. *Br J Ophthalmol* 2009;93:634-7.
59. Wang XJ, Milner TE, Nelson JS. Characterization of fluid flow velocity by optical Doppler tomography. *Opt Lett* 1995;20:1337-9.
60. Von Websky MW, Vitz M, Raptis DA, Rosenthal R, Clavien PA, Hahnloser D. Basic laparoscopic training using the simionix LAP mentor: Setting the standards in the novice group. *J surg educ*. 2012. Accessed 11/4/2012, 2012.
61. Filipucci E, Unlu Z, Farina A, Grassi W. Sonographic training in rheumatology: A self teaching approach. *Ann rheum dis*. 2003. Accessed 11/4/2012, 2012.
62. Moreno-Montanes J, Olmo N, Garcia N, Alvarez A, Garcia-Granero M. Influence of examiner experience on the reproducibility of retinal nerve fiber thickness values using Cirrus and Stratus OCTs. *J glaucoma*. 2011. Accessed 11/4/2012, 2012.
63. Pokroy R, Du E, Alzaga A, et al. Impact of simulator training on resident cataract surgery. *Graefes Arch Clin Exp Ophthalmol*. 2012. Accessed 11/4/2012, 2012.
64. Bonilha HS, Humphries K, Blair J, et al. Radiation exposure time during MBSS: Influence of Swallowing Impairment Severity, Medical Diagnosis, Clinician Experience, and Standardized Protocol Use. *Dysphagia*. 2012. Accessed 11/4/2012, 2012.
65. Bali SJ, Hodge C, Lawless M, Roberts TV, Sutton G. Early experience with the femtosecond laser for cataract surgery. *Ophthalmology*. 2012;119(5):891-899. doi: 10.1016/j.ophtha.2011.12.025.
66. Cipriany-Dacko LM, Innerst D, Johannsen J, Rude V. Interrater reliability of the tinetti balance scores in novice and experienced physical therapy clinicians. *Arch Phys Med Rehabil*. 1997;78(10):1160-1164.

67. Fathi R, Cain P, Nakatani S, Yu HC, Marwick TH. Effect of tissue doppler on the accuracy of novice and expert interpreters of dobutamine echocardiography. *Am J Cardiol.* 2001;88(4):400-405.
68. Kiani S, Desai PH, Thirumvalavan N, et al. Endoscopic venous harvesting by inexperienced operators compromises venous graft remodeling. *Ann Thorac Surg.* 2012;93(1):11-7; discussion 17-8. doi: 10.1016/j.athoracsur.2011.06.026.
69. Niazi AU, Haldipur N, Prasad AG, Chan VW. Ultrasound-guided regional anesthesia performance in the early learning period: Effect of simulation training. *Reg Anesth Pain Med.* 2012;37(1):51-54. doi: 10.1097/AAP.0b013e31823dc340.
70. Verzini F, De Rango P, Parlani G, Panuccio G, Cao P. Carotid artery stenting: Technical issues and role of operators' experience . *Perspect Vasc Surg Endovasc Ther.* 2008;20(3):247-257. doi: 10.1177/1531003508323733.
71. Huang J, Pesudovs K, Yu A, et al. A comprehensive comparison of central corneal thickness measurement *Optom Vis Sci.* 2011;88(8):940-949.
72. Ishibazawa A, Igarashi S, Hanada K, et al. Central corneal thickness measurements with fourier-domain optical coherence tomography versus ultrasonic pachymetry and rotating scheimpflug camera *Cornea.* 2011;30(6):615-619.
73. Nam SM, Im CY, Lee HK, Kim EK, Kim TI, Seo KY. Accuracy of RTVue optical coherence tomography, pentacam, and ultrasonic pachymetry for the measurement of central corneal thickness *Ophthalmology.* 2010;117(11):2096-2103.
74. Rao HL, Kumar AU, Kumar A, et al. Evaluation of central corneal thickness measurement with RTVue spectral domain optical coherence tomography in normal subjects *Cornea.* 2011;30(2):121-126.

75. Gonzalez-Garcia AO, Vizzeri G, Bowd C, Medeiros FA, Zangwill LM, Weinreb RN. Reproducibility of RTVue retinal nerve fiber layer thickness and optic disc measurements and agreement with stratus optical coherence tomography measurements *Am J Ophthalmol.* 2009;147(6):1067-74, 1074.e1.
76. Russell I. Evaluating new surgical procedures *BMJ.* 1995;311(7015):1243-1244.
77. Garas A, Vargha P, Hollo G. Reproducibility of retinal nerve fiber layer and macular thickness measurement with the RTVue-100 optical coherence tomograph *Ophthalmology.* 2010;117(4):738-746.
78. Garcia JP,Jr, Garcia PT, Rosen RB. Retinal blood flow in the normal human eye using the canon laser blood flowmeter *Ophthalmic Res.* 2002;34(5):295-299.
79. Giani A, Cigada M, Choudhry N, et al. Reproducibility of retinal thickness measurements on normal and pathologic eyes by different optical coherence tomography instruments *Am J Ophthalmol.* 2010;150(6):815-824.
80. Li JP, Wang XZ, Fu J, Li SN, Wang NL. Reproducibility of RTVue retinal nerve fiber layer thickness and optic nerve head measurements in normal and glaucoma eyes *Chin Med J (Engl).* 2010;123(14):1898-1903.
81. Ramsay CR, Wallace SA, Garthwaite PH, Monk AF, Russell IT, Grant AM. Assessing the learning curve effect in health technologies. lessons from the nonclinical literature *Int J Technol Assess Health Care.* 2002;18(1):1-10.

82. Riva CE, Grunwald JE, Sinclair SH, Petrig BL. Blood velocity and volumetric flow rate in human retinal vessels *Invest Ophthalmol Vis Sci*. 1985;26(8):1124-1132.
83. Klein R, Renaud JM, Ziadi MC, Thorn SL, Adler A, Beanlands RS, deKemp RA. Intra- and inter-operator repeatability of myocardial blood flow and myocardial flow reserve measurements using rubidium-82 pet and a highly automated analysis program. *J Nucl Cardiol*. 010;17(4):600-616.
84. Advanced Imaging for Glaucoma Study. AIGS Manual of Procedures 8.1. Available at: <http://www.aigstudy.net/index.php?id=12>. Accessibility verified January 2, 2013.
85. Kelley C, D'Amore P, Hechtman HB, Shepro D. Microvascular pericyte contractility in vitro: Comparison with other cells of the vascular wall *J Cell Biol*. 1987;104(3):483-490.
86. Burgansky-Eliash Z, Wollstein G, Chu T, et al. Optical coherence tomography machine learning classifiers for glaucoma detection: a preliminary study. *Invest Ophthalmol Vis Sci*. 2005;46:4147-4152.
87. Huang ML, Chen HY. Development and comparison of automated classifiers for glaucoma diagnosis using Stratus optical coherence tomography. *Invest Ophthalmol Vis Sci*. 2005;46:4121-4129.
88. Naithani P, Sihota R, Sony P, et al. Evaluation of optical coherence tomography and Heidelberg retinal tomography parameters in detecting early and moderate glaucoma. *Invest Ophthalmol Vis Sci*. 2007;48:3138-3145.
89. Anton A, Moreno-Montanes J, Blazquez F, et al. Usefulness of optical coherence tomography parameters of the optic disc and the retinal nerve fiber layer to differentiate glaucomatous, ocular hypertensive, and normal eyes. *J Glaucoma*. 2007;16:1-8.

90. Anton A, Castany M, Pazos-Lopez M, et al. Reproducibility of measurements and variability of the classification algorithm of Stratus OCT in normal, hypertensive, and glaucomatous patients. *Clin Ophthalmol*. 2009;3:139-145.
91. Mesiwala NK, Pekmezci M, Porco TC, et al. Optic disc parameters from Optovue optical coherence tomography: Comparison of manual versus automated disc rim determination. *J Glaucoma*. 2012;21(6):367-371.
92. Schuman JS, Wollstein G, Farra T, et al. Comparison of optic nerve head measurements obtained by optical coherence tomography and confocal scanning laser ophthalmoscopy. *Am J Ophthalmol*. 2003;135:504–512.
93. Frankel R, Altschuler A, George S, et al. Effects of Exam-Room Computing on Clinician-Patient Communication. *J Gen Intern Med*. 2005;20(8):677-682.
94. Rutherford-Hemming T. Learning in simulated environments: effect on learning transfer and clinical skill acquisition in nurse practitioner students. *J Nurs Educ*. 2012;51(7):403-406.
95. Farfel A, Hardoff D, Afek A, et al. Effect of a simulated patient-based educational program on the quality of medical encounters at military recruitment centers. *IMAJ*. 2010;12:455-459.
96. Bernad SI, Romeo SR, Bernad E, Gaita D, Mihalas GI, Munteanu I. Computerized Study of the Blood Flow in Arterial Stenosis. *Timisoara Medical Journal*. 2004;54(2):142-145.
97. Riva CE, Schmetterer, L. Microcirculation of the Ocular Fundus. *Compr Physiol*. 2011:735-765.
98. Korzon-Burakowska, A, Edmonds, M. Role of the Microcirculation in Diabetic Foot Ulceration. *International Journal of Lower Extremity Wounds*. 2006;5:144-148.

99. Wang NK, Lai CC, Chu HY, et al. Classification of early dry-type myopic maculopathy with macular choroidal thickness. *Am J Ophthalmol*. 2012;153(4):669-677.
100. Khuu LA. Retinal Blood Flow and Markers of Vascular Inflammation and Endothelial Dysfunction in Type 2 Diabetes [master's thesis]. Waterloo, ON: University of Waterloo; 2010.
101. Burgoyne CF. Image analysis of optic nerve disease. *Eye (Lond)*. 2004;18(11):1207-13.
102. Chiang A, Witkin AJ, Regillo CD, Ho AC. Fundus Imaging of Age-Related Macular Degeneration. *Age-related Macular Degeneration Diagnosis and Treatment*. 2011:39-64.
103. Song C. High-resolution high-speed spectral domain optical coherence tomography. *2009 International Symposium on Optomechatronic Technologies*. 2009:11-15.
104. Gilmore ED. Retinal Blood Flow and Vascular Reactivity in Diabetic Retinopathy [PhD thesis]. Waterloo, ON: University of Waterloo;2006.
105. Samarawickrama C, Pai A, Huynh SC, et al. Influence of OCT Signal Strength on Macular, Optic Nerve Head, and Retinal Nerve Fiber Layer Parameters. *Invest Ophthalmol Vis Sci*. 2010;51(9):4471-4475.
106. Hwang JC, Konduru R, Zhang X, et al. Relationship among Visual Field, Blood Flow, and Neural Structure Measurements in Glaucoma. *Invest Ophthalmol Vis Sci*. 2012;53(6):3020-3026.
107. Burgansky-Eliash Z, Wollstein G, Chu T, et al. Optical coherence tomography machine learning classifiers for glaucoma detection: a preliminary study. *Invest Ophthalmol Vis Sci*. 2005;46(11):4147-52.

108. Oner V, Aykut V, Tas M, et al. Effect refractive status on peripapillary retinal nerve fiber layer thickness: a study by RTVue spectral domain optical coherence tomography. *Br J Ophthalmol*. 2013;97(1):75-9.
109. Garas A. Structural evaluation of retinal ganglion cell damage: Fourier-domain optical coherence tomography and scanning laser polarimetry in glaucoma and acute optic neuritis[PhD thesis]. Budapest: Semmelweis University; 2011.
110. Fine I, Jacobs RA. Comparing perceptual learning tasks: a review. *J Vis*. 2002;2(2):190-203.
111. Beard BL, Levi DM, Reich LN. Perceptual learning in parafoveal vision. *Vision Res*. 1995;35(12):1679-90.
112. McKee SP, Westheimer G. Improvement in vernier acuity with practice. *Percept Psychophys*. 1978;24(3):258-62.
113. Chung ST, Legge GE, Cheung SH. Letter-recognition and reading speed in peripheral vision benefit from perceptual learning. *Vision Res*. 2004;44(7):695-709.
114. A Karni, D Sagi. The time course of learning a visual skill. *Nature*. 1993;365(6443):250-2.
115. Faul F, Erdfelder E, Buchner A, Land AG. Statistical power analyses using G*Power 3.1: Tests for correlation and regression analyses. *Behavior Research Methods*. 2009;41:1149-1160.

Copyright permissions

Copyright Statement

Copyright permissions have been obtained permitting me to include my published work in this thesis. For all copyright permissions inquiries, questions or comments, please email cuppal@uwaterloo.ca.

Nature Publishing Group

NATURE PUBLISHING GROUP LICENSE
TERMS AND CONDITIONS
Dec 09, 2013

This is a License Agreement between Chitman S Uppal ("You") and Nature Publishing Group ("Nature Publishing Group") provided by Copyright Clearance Center ("CCC"). The license consists of your order details, the terms and conditions provided by Nature Publishing Group, and the payment terms and conditions.

All payments must be made in full to CCC. For payment instructions, please see information listed at the bottom of this form.

License Number	*****
License date	Dec 09, 2013
Licensed content publisher	Nature Publishing Group
Licensed content publication	Eye
Licensed content title	Orbital vascular anatomy
Licensed content author	S S Hayreh
Licensed content date	Oct 4, 2006
Volume number	20
Issue number	10
Type of Use	reuse in a dissertation / thesis
Requestor type	academic/educational
Format	Electronic
Portion	figures/tables/illustrations
Number of figures/tables/illustrations	1
High-res required	No
Figures	Figure 7 A diagrammatic representation of anastomoses of the ophthalmic artery with various branches of the external carotid

Author of this NPG article	artery No
Your reference number	
Title of your thesis / dissertation	Doppler SD-OCT Blood Flow Analysis and Extraneous Operator Influences
Expected completion date	Jan 2014
Estimated size (number of pages)	70
Total	0.00 USD
Terms and Conditions	

Terms and Conditions for Permissions

Nature Publishing Group hereby grants you a non-exclusive license to reproduce this material for this purpose, and for no other use, subject to the conditions below:

1. NPG warrants that it has, to the best of its knowledge, the rights to license reuse of this material. However, you should ensure that the material you are requesting is original to Nature Publishing Group and does not carry the copyright of another entity (as credited in the published version). If the credit line on any part of the material you have requested indicates that it was reprinted or adapted by NPG with permission from another source, then you should also seek permission from that source to reuse the material.
2. Permission granted free of charge for material in print is also usually granted for any electronic version of that work, provided that the material is incidental to the work as a whole and that the electronic version is essentially equivalent to, or substitutes for, the print version. Where print permission has been granted for a fee, separate permission must be obtained for any additional, electronic re-use (unless, as in the case of a full paper, this has already been accounted for during your initial request in the calculation of a print run). NB: In all cases, web-based use of full-text articles must be authorized separately through the 'Use on a Web Site' option when requesting permission.
3. Permission granted for a first edition does not apply to second and subsequent editions and for editions in other languages (except for signatories to the STM Permissions Guidelines, or where the first edition permission was granted for free).
4. Nature Publishing Group's permission must be acknowledged next to the figure, table or abstract in print. In electronic form, this acknowledgement must be visible at the same time as the figure/table/abstract, and must be hyperlinked to the journal's homepage.
5. The credit line should read:

Reprinted by permission from Macmillan Publishers Ltd: [JOURNAL NAME] (reference citation), copyright (year of publication)

For AOP papers, the credit line should read:

Reprinted by permission from Macmillan Publishers Ltd: [JOURNAL NAME], advance online publication, day month year (doi: 10.1038/sj.[JOURNAL ACRONYM].XXXXX)

Note: For republication from the *British Journal of Cancer*, the following credit lines apply.

Reprinted by permission from Macmillan Publishers Ltd on behalf of Cancer Research UK: [JOURNAL NAME] (reference citation), copyright (year of publication) For AOP papers, the credit line should read:

Reprinted by permission from Macmillan Publishers Ltd on behalf of Cancer Research UK: [JOURNAL NAME], advance online publication, day month year (doi: 10.1038/sj.[JOURNAL ACRONYM].XXXXX)

6. Adaptations of single figures do not require NPG approval. However, the adaptation should be credited as follows:

Adapted by permission from Macmillan Publishers Ltd: [JOURNAL NAME] (reference citation), copyright (year of publication)

Note: For adaptation from the *British Journal of Cancer*, the following credit line applies.

Adapted by permission from Macmillan Publishers Ltd on behalf of Cancer Research UK: [JOURNAL NAME] (reference citation), copyright (year of publication)

7. Translations of 401 words up to a whole article require NPG approval. Please visit <http://www.macmillanmedicalcommunications.com> for more information. Translations of up to a 400 words do not require NPG approval. The translation should be credited as follows:

Translated by permission from Macmillan Publishers Ltd: [JOURNAL NAME] (reference citation), copyright (year of publication).

Note: For translation from the *British Journal of Cancer*, the following credit line applies.

Translated by permission from Macmillan Publishers Ltd on behalf of Cancer Research UK: [JOURNAL NAME] (reference citation), copyright (year of publication)

We are certain that all parties will benefit from this agreement and wish you the best in the use of this material. Thank you.

Special Terms:

v1.1

If you would like to pay for this license now, please remit this license along with your payment made payable to "COPYRIGHT CLEARANCE CENTER" otherwise you will be invoiced within 48 hours of the license date. Payment should be in the form of a check or money order referencing your account number and this invoice number RLNK501178129.

Once you receive your invoice for this order, you may pay your invoice by credit card. Please follow instructions provided at that time.

**Make Payment To:
Copyright Clearance Center
Dept 001
P.O. Box 843006
Boston, MA 02284-3006**

For suggestions or comments regarding this order, contact RightsLink Customer Support: customer care@copyright.com or +1-877-622-5543 (toll free in the US) or +1-978-646-2777.

Gratis licenses (referencing \$0 in the Total field) are free. Please retain this printable license for your reference. No payment is required.

Pilot Study

Doppler SD-OCT blood flow analysis and extraneous operator and grader influences : A pilot Study

CS. Uppal, C. Hudson

Retina Research Group, School of Optometry and Vision Science, University of Waterloo

Purpose: This study investigated the presence of any learning effects associated with novice and experienced image acquisition and novice and experienced image grading, using a RTVue SD-OCT system.

Methods: Five males and 5 females were recruited in this study. One eye of each of 10 healthy young (mean age 25.8; SD 2.7 years; ranging from 22 to 30 years) subjects was randomly selected for the study and the pupil was dilated using Mydracyl 1%. SD-OCT Doppler blood flow was non-invasively measured using the RTVue system (Optovue Inc., USA). A double circular scanning pattern was employed. A minimum of six separate SD-OCT Doppler measurements (i.e. each measurement comprising an upper and lower nasal pupil scan) were acquired. Measurements were repeated on a second and third visit. Retinal blood flow (RBF) was calculated, using data from valid scans only, by summing flow from all detectable venules.

Results: 22 of 24 images (91.67%) were determined to be valid using the DOCTORC software (Centre for Ophthalmic Optics and Lasers, CA, USA). Mean total RBF from the first visit was found to be $57.11 \pm 2.02 \mu\text{l}/\text{min}$ by an experienced grader. This result must be compared with experienced image acquisition and grading to determine if any learning effects lie within acquisition. Ideally, there should be a statistically significant difference ($p < 0.05$) between the blood flow parameters provided by novice image acquisition and grading compared with experienced image acquisition and grading.

Conclusions: Analyses will be made based upon the comparison of all novice operator-grader relationships to experienced image acquisition and grading. The relatively small sample size should be considered when interpreting these results.